View metadata, citation and similar papers at core.ac.uk

brought to you by CORE

provided by Carolina Digital Repository

Cerebral Cortex December 2010;20:2900–2915
doi:10.1093/cercor/bhq039
Advance Access publication March 22, 2010

Nociceptive Afferent Activity Alters the SI RA Neuron Response to Mechanical Skin Stimulation

B.L. Whitsel[1,2], O.V. Favorov[1], Y. Li[1,3], J. Lee[1], P.M. Quibrera[2] and M. Tommerdahl[1]

[1]Department of Biomedical Engineering and [2]Department of Cell and Molecular Physiology, University of North Carolina, Chapel Hill, NC 27599, USA

[3]Current address: Research Engineering Laboratory, Memorial Sloan-Kettering Cancer Center, New York, NY 10065, USA

Address correspondence to B.L. Whitsel. Email: bwhitsel@med.unc.edu.

Procedures that reliably evoke cutaneous pain in humans (i.e., 5–7 s skin contact with a 47–51°C probe, intradermal algogen injection) are shown to decrease the mean spike firing rate (MFR) and degree to which the rapidly adapting (RA) neurons in areas 3b/1 of squirrel monkey primary somatosensory cortex (SI) entrain to a 25-Hz stimulus to the receptive field center (RF_{center}) when stimulus amplitude is "near-threshold" (i.e., 10–50 μm). In contrast, RA neuron MFR and entrainment are either unaffected or enhanced by 47–51 °C contact or intradermal algogen injection when the amplitude of 25-Hz stimulation is 100–200 μm (suprathreshold). The results are attributed to an "activity dependence" of γ-aminobutyric acid (GABA) action on the $GABA_A$ receptors of RA neurons. The nociceptive afferent drive triggered by skin contact with a 47–51 °C probe or intradermal algogen is proposed to activate nociresponsive neurons in area 3a which, via corticocortical connections, leads to the release of GABA in areas 3b/1. It is hypothesized that GABA is hyperpolarizing/inhibitory and suppresses stimulus-evoked RA neuron MFR and entrainment whenever RA neuron activity is low (as when the RF_{center} stimulus is weak/near-threshold) but is depolarizing/excitatory and augments MFR and entrainment when RA neuron activity is high (when the stimulus is strong/suprathreshold).

Keywords: bipolar GABA action, interareal interactions, mechanoresponsivity, pain–touch interaction, primary somatosensory cortex, vibrotactile frequency discrimination

Introduction

Human studies (healthy subjects—Apkarian et al. 1992, 1994; Maxfield and Bolanowski 1994, 1995; Bolanowski 1996; Bolanowski et al. 2000, 2001 chronic pain patients—Hollins et al. 1996, 2001; Hollins and Sigurdsson 1998) have demonstrated that clinical pain or experimentally evoked nociceptor afferent activity is accompanied by significant degradation not only of the perceptual abilities to detect vibrotactile stimulation but also to discriminate vibrotactile stimuli that differ only in frequency. Consistent with these observations are results indicating that pain or skin nociceptor afferent drive is accompanied by "suppression/inhibition" of the primary somatosensory cortical (SI) response to skin stimuli that preferentially activate rapidly conducting (A_β) mechanoreceptive afferents. As examples, Tran et al. (2003) observed that painful electrical stimulation of the skin is accompanied by a decreased amplitude of the early magnetic fields evoked in SI by electrical stimulation of A_β afferents, and Apkarian et al. (Apkarian et al. 1992, 1994) used functional imaging methods to show that the human contralateral SI response to a spatially discrete tactile stimulus is reduced in the presence of thermal pain experienced at the same or a nearby skin site. Also consistent with the idea that pain/nociceptive afferent drive exerts a suppressive/inhibitory effect of pain on the SI response to A_β mechanoreceptor afferent drive is the finding that transection of the spinothalamic tract at a cervical level of the spinal cord in patients with chronic pain is followed not only by pain relief but also by an increase of the amplitude of the short-latency potentials evoked in the contralateral areas 3b and 1 by stimuli that selectively activate A_β afferents (Rosso et al. 2003).

Observations reported in other human studies make it clear, however, that the effects of pain/nociceptor afferent drive on tactile perception and central nervous system (CNS) processing/representation of tactile stimuli are not explicable solely in terms of pain/nociceptor-evoked central inhibition. As examples, laser-applied stimuli which evoke activity in nociceptive skin afferents facilitate the SI magnetoencephalographic response to A_β afferent input (Ploner et al. 2004); tactile "hyperesthesia" occurs in normal healthy subjects following an exposure to experimentally induced skin pain (Svensson et al. 1998); perceptual responsivity to localized mechanical skin stimulation is increased in the presence of temporomandibular joint pain (Ayesh et al. 2007) or after third molar extraction (Eliav and Gracely 1998); the SI functional magnetic resonance imaging (fMRI) response to a spatially localized tactile stimulus is increased following intradermal capsaicin injection in normal subjects (Iadarola et al. 1998; Baron et al. 1999, 2000; Maihofner et al. 2004, 2005; Peyron et al. 2004); and finally, although both fMRI activity in contralateral SI somatosensory cortex and vibrotactile sensitivity on the forearm decrease substantially and significantly during painful thermomechanical contact of a small (21 mm^2) region on the hand, painful thermomechanical contact with a more extensive (1074 mm^2) area on the hand is accompanied by increased fMFRI activity in the contralateral SI and, also unlike the decrease of vibrotactile sensitivity obtained with localized painful thermomechanical contact, vibrotactile sensitivity in the presence of such large-area thermomechanical contact is unchanged (Apkarian et al. 2000).

The experiments described in this paper were undertaken in an attempt to obtain information that would enable straightforward neuromechanistic explanation of the above-described diverse and seemingly conflicting effects of pain/nociceptor afferent drive on the SI response to tactile stimulation and tactile perception. More specifically, the experiments of the present study sought to evaluate the possibility that the effect of pain/nociceptor afferent drive (suppression or enhancement) on the SI response to A_β mechanoreceptor afferent

© The Author 2010. Published by Oxford University Press. All rights reserved.
For permissions, please e-mail: journals.permissions@oxfordjournals.org

drive, and thus on tactile perception, might depend on the parameters of the mechanical skin stimulus. The present study focused on stimulus strength/intensity as a possible determinant of the sign/polarity of cortical tactile–pain interaction. To this end, we evaluated the impact of 2 manipulations (i.e., 5–7 s skin contact with a 47–51 °C probe—Li et al. 2001, 2002; intradermal algogen injection—Szolcsanyi 1987; LaMotte et al. 1992; Torebjork et al. 1992; α,β-methylene-adenosine 5′-triphosphate—Hamilton et al. 1999, 2000, 2001) on the response of SI cortical cutaneous mechanoresponsive neurons to near-threshold versus suprathreshold vibrotactile (25 Hz) stimulation of the receptive field (RF).

Some of the findings were described previously in preliminary communications (Li et al. 2001, 2002; Lee et al. 2009; Whitsel, Favorov, Li, Lee, and Tommerdahl 2009).

Materials and Methods

Subjects

An institutional review committee reviewed all procedures involving animal subjects in advance of the initiation of experiments. All procedures were in full compliance with National Institutes of Health policy on animal welfare. Subjects were 10 adult male and female squirrel monkeys (*Saimiri sciureus*).

Subject Preparation

General anesthesia was induced with 4% isofluorane in a 50/50 mixture of oxygen and N_2O. Following tracheal intubation the anesthetic gas mix (1–3% isofluorane in a 50/50 mixture of oxygen and N_2O) was delivered via an anesthesia machine (Forreger Compac-75) connected via flexible tubing to the tracheal cannula. A polyethylene cannula inserted into the hindlimb femoral vein enabled administration of drugs, glucose (5%), and electrolytes (0.9% saline). Methylprednisolone sodium succinate (20 mg/kg) and gentamicin sulfate (2.5 mg/kg) were injected intramuscularly to protect against cerebral edema and bacterial septicemia, respectively.

A trephine and rongeurs were used to make a 1–1.5 cm^2 opening in the skull overlying SI cortex. A Lexan recording chamber was placed over the opening and attached to the skull with dental acrylic. Wound margins outside the recording chamber were infiltrated with a long-lasting local anesthetic (Cetacaine) and closed with sutures, the dura overlying SI was incised and removed, and skeletal neuromuscular transmission blocked using intravenous (i.v.) Norcuron (loading dose: 0.25–0.5 mg/kg; maintenance dose: 0.025–0.05 mg/kg/h).

Following completion of the above-described surgical procedures a 50/50 mix of N_2O and oxygen was delivered to the subject via a positive pressure ventilator. The concentration of isofluorane in the anesthetic gas mix was adjusted as needed (typically to values between 0.5% and 1.0%) to ensure that heart rate, blood pressure, and the slow-wave content of the electroencephalogram remained at values consistent with general anesthesia. End-tidal CO_2 was maintained between 3.0% and 4.5% by varying the rate and depth of ventilation; rectal temperature was monitored (using a rectal probe) and maintained between 36.5 and 38 °C using an electronically controlled heating pad that remained in contact with the subject's abdomen and chest throughout the experiment. Euthanasia was accomplished by i.v. injection of pentobarbital (50 mg/kg) and by intracardial perfusion with saline followed by fixative (10% formalin).

Thermotactile Stimulation

The stimulator used in all experiments (CS-540 Thermo-Vibrotactile Stimulator, Cantek Enterprises) enables concurrent delivery of precisely controlled thermal and vibrotactile stimulation to a discrete skin site. Stimulator contact with the subject's skin was via the tip of a cylindrical metal contactor probe (5-mm diameter). Stimulator probe temperature was altered and maintained at an investigator-specified value by varying the flow rates (via software-controlled valves) of hot and cold water from 2 constant-temperature baths (RTE-211, Netlab Inc.) connected to the stimulator via insulated tubing.

The long axis of the stimulator probe was positioned perpendicular to the skin with the tip at a position ~5 mm above the skin site to be stimulated. Only after heating the probe to the desired temperature did the stimulator's control system advance the probe to indent the skin by ~1 mm. Following 50–100 ms of stationary contact at this depth, sinusoidal vertical oscillation of the probe was initiated at a frequency of 25 Hz. The peak-to-peak amplitude of the oscillation was investigator-specified—in the experiments described in this paper, 25-Hz vertical displacement stimulation was applied to the neuron's receptive field center (RF_{center}) at 1–4 amplitudes selected from within the range of 10–200 μm. The probe remained in contact with the skin throughout each stimulus trial (typically 5 s). All stimuli were delivered to a site on the contralateral volar hand.

Throughout the period of 25-Hz stimulation, the temperature of the stimulator probe was maintained at: 1) a temperature between 25 and 38 °C—normal conscious human subjects experience static 5–7 s probe contact with the skin at a temperature within this range as "thermoneutral"/"nonpainful" and assign the sensation a value of "0" using a 10-point pain rating scale where 0 indicates no pain and 10 indicates unbearable pain; 2) 47 °C—subjects rate 5–7 s static probe contact with the skin at this temperature as "warm/marginal pain," corresponding to values between 1 and 2 using the same pain rating scale; 3) 48 °C—probe contact with the skin for 5–7 s at this temperature is rated by conscious subjects as "marginally painful" and assigned a value between 2 and 3; or 4) a temperature between 49 and 51 °C—contact at a temperature within this range is rated as "moderately painful" and assigned a value between 4 and 5 (Vierck et al. 1997; Whitsel, Favorov, Li, Quibrera, and Tommerdahl 2009).

The stimulator probe was retracted to a position ~5 mm above the skin and maintained at that position: 1) for 30 s after each 5- to 7-s stimulus trial delivered during the CONTROL, TEST, and RECOVERY phases (each phase consisted of 4–6 trials) of the 2 stimulation protocols (described in subsequent section entitled "stimulation protocols") and 2) for 3 min after the last trial of the CONTROL, TEST, and RECOVERY phases of the protocol. Successive stimulation protocols were separated by an interval of at least 5 min during which no stimuli were presented. When delivered to a site on the skin of the distal forearm or hand of the authors, the protocols/stimuli described in this paper never evoked escape, persisting alterations of tactile sensation, or visually apparent skin damage. A time-of-day referenced digital record (sampling rate 20 KHz) of probe position, probe temperature, and neuronal spike firings was created for each experiment and stored as an electronic file.

OIS Imaging

The near-infrared optical intrinsic signal (OIS) imaging method, used previously by the authors to study the SI cortical response to nonnoxious mechanical and noxious skin heating stimulation (Tommerdahl et al. 1996, 1998, 1999), was used in the initial phase of all experiments. The OIS images generated in this way guided placement of the microelectrode penetrations performed in the subsequent neurophysiological recording phase of the experiment. Availability of images of the OIS response of the subject's SI cortex to the same stimulus conditions used to study the spike firing response of individual SI mechanoresponsive neurons ensured that extracellular recordings of spike discharge activity were obtained from neurons in the cortical region which in that subject responded maximally to 25-Hz vibrotactile stimulation.

Neurophysiological Recording

Electrodes, Recording Conditions

Extracellular recordings of the spike discharge activity of single neurons or small SI neuron groupings (typically consisting of the activity of 2–5 neurons) were obtained using electrolytically etched, glass-insulated tungsten wires (impedance 300–500 kΩ at a test frequency of 10 kHz). To minimize the cortical and vascular movements associated with the cardiac and respiratory cycles, each

microelectrode penetration was carried out under "closed-chamber" conditions—achieved by filling the recording chamber with artificial cerebrospinal fluid and hydraulically sealing it with a glass plate containing an "o-ring" through which the microelectrode was advanced under direct visual control.

Neuron Classification

Of the multiple classes of cutaneous mechanoresponsive neurons that occupy areas 3b and 1, only those neurons dominated by input from the RA-I class of rapidly adapting skin afferents (i.e., identified as "RA" neurons in this paper) were targeted for in-depth evaluation. The authors view restriction of the analyses described in this paper to the spike train activity of members of this SI neuron subpopulation as consistent with our goal of improving the currently deficient neuromechanistic understanding of the impact of pain on tactile perception. Particularly influential in this decision were published findings that have established that: 1) it is the spike discharge activity of the SI RA neurons which underlies the perceptual abilities of humans and animal subjects to discriminate vibrotactile stimuli differing solely in frequency within the frequency range 10–50 Hz (Mountcastle et al. 1969, 1990; LaMotte and Mountcastle 1975, 1979; Hernandez et al. 2000) and 2) either clinical pain or experimentally induced nociceptor afferent drive degrades the normal human capacities not only to detect but also to discriminate 10- to 50-Hz vibrotactile stimulation (Apkarian et al. 1992, 1994; Maxfield and Bolanowski 1995; Bolanowski 1996; Hollins et al. 1996, 2001; Hollins and Sigurdsson 1998; Bolanowski et al. 2000, 2001).

Skin mechanoresponsive SI neurons were identified initially using handheld mechanical "search" stimuli (e.g., skin brushing, tapping, vibration, and static skin indentation). Only after positive identification of a neuron as a member of the RA class of SI mechanoresponsive neurons (Sur et al. 1984; Bensmaia et al. 2006) was the thermovibrotactile stimulator set up and employed to deliver series of precisely controlled static indentation stimuli to the skin site identified as the neuron's RF_{center}. The neuronal spike activity evoked by such stimuli enabled confirmation/rejection of the investigator's initial classification based on the neuron's response to handheld mechanical stimuli.

Stimulation Protocols

The Standard 3-Phase Protocol

Three series of 25-Hz vibrotactile stimuli were delivered using this protocol. All stimuli (typically 4–6) in the initial series (CONTROL) were delivered with the stimulator probe preheated to 38 °C. Next, a second series (TEST) of stimuli identical in all respects except one was delivered to the same skin site—that is, during this second series of stimuli the probe of the stimulator was maintained at a temperature selected from within the range 47–51 °C. A final (third; RECOVERY) series of stimuli then was reapplied to the same site with the stimulator probe again at 38 °C. In all trials and in all phases of this protocol, the same duration of 25-Hz stimulation was used, and a 30-s interstimulus interval always separated successive control, test, or recovery stimuli. A 3-min no-stimulus delay separated the CONTROL, TEST, and RECOVERY series of stimuli delivered in the same run.

The Multiple Amplitude Protocol

The effect of noxious skin heating on the response of a limited sample (n = 12) of RA neurons to 25 Hz stimulation of the RF_{center} was studied using a protocol substantially more lengthy than the above-described 3-phase (standard) protocol. Like the standard protocol, the multiple-amplitude protocol delivered 25-Hz stimuli to the RF_{center} at a probe temperature selected from within the range 25–38 °C and also between 47 and 51 °C. Unlike the standard protocol, the multiple-amplitude protocol delivered 25-Hz stimulation to the RF_{center} at each of a series of amplitudes (typically 3–5) that included near-threshold as well as suprathreshold values. The different amplitudes of 25-Hz stimulation were delivered in randomized order in the CONTROL, TEST, and RECOVERY phases of this protocol.

Neural Data Analysis

Custom-made software allowed postexperimental display and review of the digital records of neuronal spike firing and stimulator events collected and stored during an experiment. The spike firing activity was reviewed using a high-resolution monitor, and the activity attributed to individual (SU) or small neuron groupings (MURs) was discriminated on the basis of amplitude using voltage windows. Multiple (typically 2–3) nonoverlapping voltage windows were identified at each recording site. An output data file registered the times of occurrence of the action potentials falling within each voltage window and also the times of specific stimulator events (onset and offset of each sinusoidal cycle, etc.).

2 aspects of SI neuron spike discharge activity were evaluated: 1) mean spike firing rate (MFR) per second and 2) entrainment ("R"; for description of the method for calculation of R see Whitsel, Favorov et al. 2000; Whitsel, Kelly et al. 2000; Whitsel et al. 2001, 2003). The R measure quantifies the extent to which spike discharge is phase-locked to the sinusoidal motion of the stimulator: the value of R can vary between 0, indicating random organization of spike discharge activity within the stimulus cycle, and 1, indicating perfect entrainment to the sinusoidal stimulus.

Intradermal Injection of Algogen

Extracellular recordings of the spike firing of mechanoresponsive SI neurons evoked by precisely controlled mechanical skin stimulation and in the absence of intentional stimulation were obtained before, during, and subsequent to the highly selective skin C-nociceptor afferent activation elicited by intradermal injection (using a 29-gauge hypodermic needle and 0.5-mL syringe) of 10–20 μL of a 1% capsaicin solution (LaMotte et al. 1992; Torebjork et al. 1992) or 50–100 μL of a 5 mM solution of α β me ATP in saline (Hamilton et al. 1999, 2000, 2001). The needle was inserted into a skin site 4–10 mm away from the neuron's RF_{center} 15–20 s prior to the infusion of algogen. The infusion required ≤5 s to complete, after which the needle was withdrawn. The same protocols used to characterize the response of an RA neuron to 25-Hz stimulation of the RF_{center} prior to algogen injection were used repetitively to: 1) assess the effect, if any, of algogen on that same neuron's response to such stimulation and 2) evaluate the time course of that effect.

Histological Procedures/Identification of Cytoarchitectural Boundaries

Following tissue fixation, the SI region traversed by each microelectrode was serially sectioned at 30–60 μm in the sagittal plane. The sections were stained with cresyl fast violet and inspected microscopically to distinguish anterior parietal regions on the basis of established cytoarchitectonic criteria (Powell and Mountcastle 1959; Jones and Porter 1980; Sur et al. 1982). Microscopic examination of the histological sections revealed the locations of microelectrode tracks and electrolytic lesions. The laminar locus, at which a recording of spike discharge activity was obtained, was determined for the majority of recordings of RA neuron activity (47/64) based on the micrometer reading on the microdrive used to advance the electrode to that location. For the remaining recordings (n = 17), the site of the electrode tip was marked immediately after completion of data collection by passing 1.5–5.0 μamps of DC current through the electrode, creating a discrete electrolytic lesion that subsequently could be identified by microscopic examination of the Nissl-stained histological sections (Fig. 1*B*). While the great majority (51/64 = 79.7%) of RA neurons that were studied were located in the middle cortical layers (layers III–V), neurons in layer II (n = 4) and layer VI (n = 9) also were studied.

Results

RA Neuron Identification

Figure 1*A* shows for each microelectrode penetration that yielded recordings of stimulus-evoked RA neuron spike discharge activity (n = 15), the locus at which each penetration

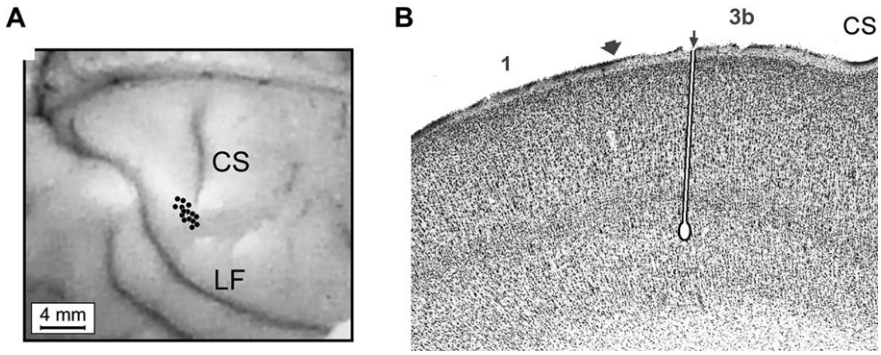

Figure 1. SI recording sites. (*A*) A photograph of surface of squirrel monkey right hemisphere. Each dot in the vicinity of the lateral end of the central sulcus (CS) shows location of microelectrode penetration that yielded recordings of area 3b/1 RA neuron spike discharge activity evoked by 25-Hz stimulation of the RF_{center} in the absence and presence of skin nociceptor afferent drive. LF, lateral fissure. (*B*) Microphotograph showing entry point (small arrow) and intracortical path (radially oriented track below small arrow) of penetration that yielded extracellular recordings of RA neuron spike discharge activity. Large filled arrow indicates location of boundary between areas 3b and 1.

made initial contact with the cortical surface. Each penetration was inserted so that it traversed the localized (1- to 2-mm diameter) zone in the hand representational region of area 3b or area 1 of the contralateral hemisphere that underwent the maximal increase in light absorbance (wavelength 830 nm; "near-infrared") in response to the 5–7 s 25-Hz vibrotactile "OIS mapping" stimulus. Each microelectrode penetration performed in the experiments described in this paper was placed within the SI region that underwent the maximal OIS in response to 25-Hz vertical skin displacement stimulation of a discrete (5-mm diameter) site on the skin of the contralateral hand. Because the magnitude of the OIS that develops in SI in response to an adequate stimulus is highly correlated with the magnitude of the stimulus-evoked increase of SI neuron spike firing activity (Tommerdahl et al. 1996, 1998, 1999; Whitsel, Favorov et al. 2000), use of this approach ensured that the RF_{center} of the great majority of the neurons encountered by the microelectrode corresponded to the skin site contacted by the stimulator probe. When it was ascertained that the RF_{center} of a neuron deviated from the locus of the "mapping stimulus," the position of stimulator probe was shifted (using a microdrive-controlled 3-axis positioner) so that the 25-Hz stimulus was delivered to the RF_{center}.

The microelectrode penetrations indicated in Figure 1*A* yielded, in addition to recordings of RA neuron activity, some recordings of the spike firing of slowly adapting (SA) mechanoresponsive SI neurons. Although the impact of elevating stimulator probe temperature to 47–51 °C on the response of SA neurons to 25-Hz stimulation of the RF_{center} also was evaluated using the same protocols used to study RA neuron spike firing behavior (the "standard" and "multiple amplitude" protocols; see Materials and Methods), description of observations obtained from SA neurons will be presented in a separate paper.

At each cortical site where the spike firing evoked by handheld mechanical search stimulation appeared consistent with the behavior of RA neurons (i.e., high sensitivity and reliable elevation of MFR in response to periodic mechanical skin stimulation, rapid adaptation of the MFR response to static contact within the RF, transient elevation of MFR to both the onset and removal of probe contact with the RF, and limited and spatially continuous RF), mechanical skin contact elicited above-background spike discharge across well-defined and spatially continuous regions on the glabrous skin of the contralateral hand. After determining that the spike activity derived either from an individual or a small grouping (2–5) of RA neurons, the laboratory's thermo-vibrotactile stimulator (described in Materials and Methods) was set up and used to deliver sinusoidal 25-Hz vertical skin displacement stimulation to the skin site identified as the RF_{center} of the responding neuron/neuronal grouping. For each such recording, the RF_{center} was a skin locus from which transient skin contact reliably triggered the most prominent elevation of MFR.

Evaluation of the Effects of 47–51 °C Skin Contact

Effects on the Response of an Exemplary RA Neuron to Near-Threshold Stimulation of the RF_{center}

The spike train records in part A of Figure 2 show that the MFR response of this area 3b RA neuron to 50 μm 25-Hz stimulation with the stimulator probe at 48 °C (trials #7–#12; the "TEST" trials) is substantially smaller than the response obtained in the "CONTROL" trials (#1–#6; the initial set of trials during which probe temperature was 38 °C). Furthermore, visual examination of the spike trains in Figure 2*A* reveals that although the magnitude of the suppression of MFR that accompanied 48 °C probe contact with this RA neuron's RF_{center} increased progressively after the onset of each trial, the suppression of MFR did not persist beyond the 30 s no-stimulus period that separated successive TEST trials (i.e., stimulus-evoked MFR during the initial 1–2 s of each TEST trial is the same as during the CONTROL trials).

The peristimulus time (PST) histograms and difference PST histograms (ΔPSTs) shown in Figure. 2*B* provide quantitative confirmation of the suggestion (derived from visual inspection of the spike trains in panel A of Fig. 2) that the suppressive influence of 48 °C probe contact on this RA neuron's MFR response to 25-Hz stimulation: 1) increased progressively with increasing time after the onset of each TEST trial (in trials #7–#12) and 2) is no longer apparent in the trials carried out subsequent to the exposure to 48 °C probe contact with the RF (during the RECOVERY trials; i.e., trials #13–#18).

In addition to undergoing a substantial decrease of the MFR associated with near-threshold 25-Hz stimulation of the RF_{center} when the temperature of the stimulator probe was increased to 48 °C, the RA neuron that yielded the observations shown in Figure 2 also underwent a substantial

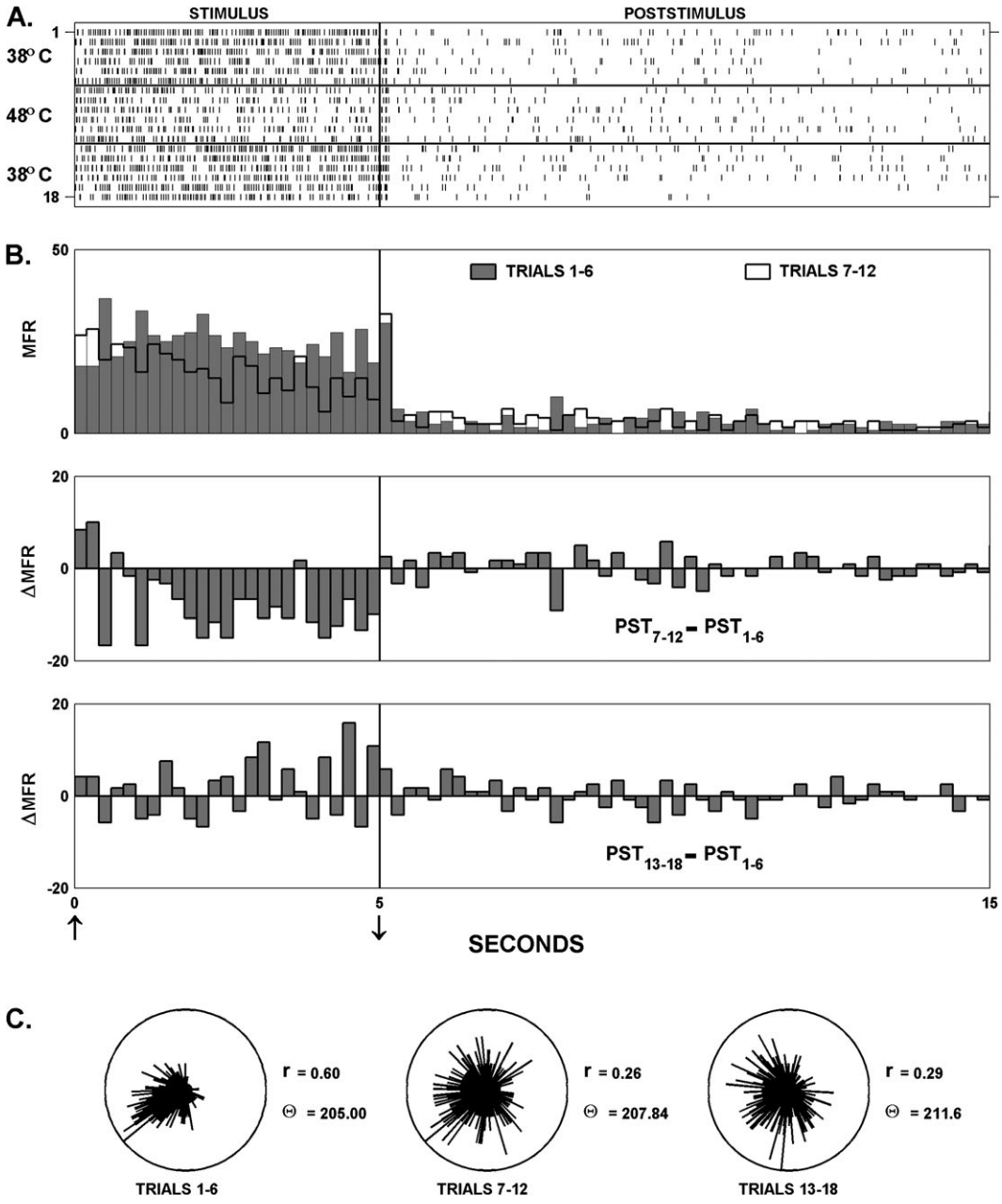

Figure 2. Response of exemplary area 3b RA neuron to 38 °C versus 48 °C near-threshold 25-Hz stimulation of the RF_{center}. (*A*) Raster-type plot showing spike trains recorded during (0–5 s) and following (5–15 s) 18 applications (trials) of a 25 Hz, 50 μm amplitude stimulus to the RF_{center}. Probe temperature during trials #1-#6 and #13-#18 was 38 °C; 48 °C during trials #7-#12. Vertical line at 5 s indicates time in each trial when stimulator probe retracted to a position 5 mm above the RF_{center}. (*B*) Top: superimposed PST histograms showing mean spike firing rate (MFR) during trials #1-#6 (shaded) and trials #7-#12 (open). Middle: difference PST histogram (ΔPST) showing difference between MFRs recorded during trials #7-#12 and #1-#6 ($PST_{7-12} - PST_{1-6}$). Bottom: ΔPST showing difference between MFRs recorded during trials #13-#18 and #1-#6 ($PST_{13-18} - PST_{1-6}$). (*C*) Circular histograms showing distribution within stimulus cycle of spike firings recorded during CONTROL (left), TEST (center), and RECOVERY trials (right).

degradation of its ability to signal stimulus frequency using a periodicity code. More specifically, the degree to which the spike activity of this neuron entrained to the 25-Hz stimulus in the trials in which the temperature of the probe was 48 °C (trials #7–#12) is considerably less than the degree of entrainment measured in the CONTROL trials (#1–#6)—see circular histograms and associated R values in part C of Figure. 2. Interestingly, this exemplary RA neuron's entrainment to 25-Hz stimulation did not recover immediately following the TEST trials—that is, entrainment to 25-Hz stimulation during the RECOVERY trials shown in Figure. 2 did not, as did stimulus-evoked MFR, recover to the values obtained in the CONTROL trials. Instead, the degree of this neuron's entrainment to 25-Hz stimulation remained subnormal for ~10 min after completion of the RECOVERY trials shown in Figure 2.

The majority (23/35 = 65.7%) of the RA neurons studied in the manner shown in Figure 2 exhibited a persisting suppression of their stimulus-evoked response after the exposure to 47–51 °C skin contact, but because this behavior varied

substantially from one neuron to the next (e.g., for some neurons both MFR and entrainment remained suppressed following the exposure to heated skin contact; for others only entrainment remained suppressed), no attempt was made to quantify this aspect of the RA neuron response to 47–51 °C skin contact.

Effects on the Response of the Same Exemplary RA Neuron to Suprathreshold Stimulation of the RF_{center}

The spike train observations and histograms in Figure 3 were obtained at a later time from the same exemplary RA neuron (at ~20 min after completion of the RECOVERY trials illustrated in Fig. 2). Unlike the substantial suppression of this neuron's MFR and entrainment to 25-Hz stimulation of the RF_{center} that occurred when the 48 °C stimulus was near-threshold (50 μm; see Fig. 2), when the amplitude of the 25-Hz stimulus was suprathreshold (200 μm) and delivered at a probe temperature of 48 °C (in trials #6–#12 of Fig. 3*A*) neither stimulus-evoked MFR nor the degree to which spike activity entrained to the stimulus differed significantly from the values obtained in the 38 °C CONTROL trials. More specifically, increasing the amplitude of the 25-Hz stimulus to 200 μm eliminated the prominent suppression by 48 °C skin contact of this exemplary RA neuron's MFR and entrained responses to 25-Hz stimulation to the RF_{center} that occurred when the stimulus amplitude was 50 μm (cf. Figs 2 and 3).

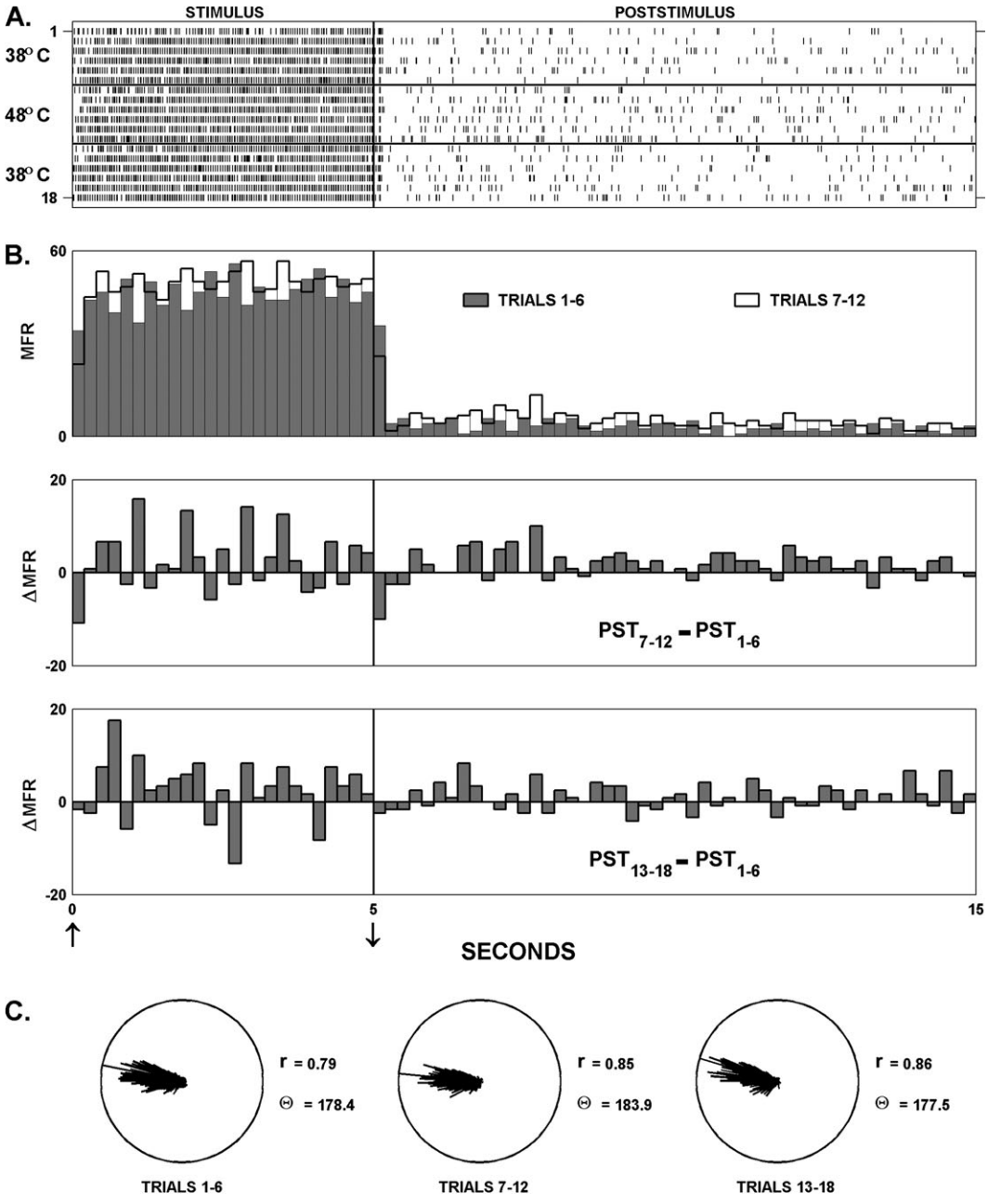

Figure 3. Effect of 48 °C skin contact on response of exemplary area 3b RA neuron to suprathreshold 25-Hz stimulation of the RFcenter. Same RA neuron, stimulation protocol, and format as in Figure 2. Observations were obtained using a suprathreshold amplitude of 25-Hz stimulation (i.e., 200 μm rather than the 50 μm amplitude used to obtain the data in Fig. 2).

Time Course of the Effect of 47–51 °C Contact on the MFR Response of SI RA Neurons to Near-Threshold 25-Hz Stimulation of the RF_{center}

The plot of ΔMFR versus time in Figure 4 shows the average across-RA neuron (n = 35) alteration of MFR that occurred when the temperature of the probe used to deliver 25-Hz stimulation to the RF_{center} was increased from a value between 25 and 38 °C to a value between 47 and 51 °C. For each of the 35 RA neurons that were studied using the standard 3-phase stimulation protocol, the MFR observed during each successive 150-ms interval during the 15-s period after stimulus onset in the CONTROL trials (averaged across trials) was subtracted from the MFR during the same temporal interval in the TEST trials. Accordingly, a negative ΔMFR value in the plot in Figure. 4 indicates that during this temporal interval RA neuron MFR was suppressed, whereas a positive ΔMFR value indicates that RA neuron MFR was enhanced.

The principal attributes of the effect of skin contact with a 47–51 °C probe on the SI RA neuron MFR response to near-threshold (10–50 μm) 25-Hz stimulation of the RF_{center} are as follows (see Fig. 4). First, the MFR response of RA neurons to near-threshold 25-Hz stimulation underwent a significant suppression (P < 0.001) during the period of 47–51 °C probe contact with the RF_{center} (see also Fig. 5*A*). Second, subsequent to termination (at 5 s) of the exposure to the near-threshold 47–51 °C 25-Hz stimulus, MFR initially remained below-normal for ~3.8 s after the probe was removed from the skin (relative to the MFR observed during the same temporal interval in the CONTROL trials; estimated using the X-intercept of the regression equation for the data obtained between 5 and 10 s after stimulus onset; P < 0.0001) but thereafter underwent a transient facilitation before reattaining values similar to those observed at the corresponding time in the CONTROL trials.

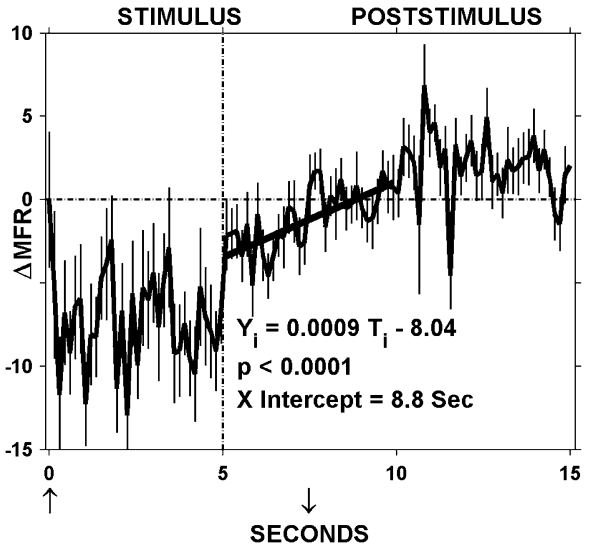

Figure 4. Effect of 47–51 °C contact on RA neuron MFR response. Average across-RA neuron (n = 35) MFR alteration (ΔMFR) during and following onset of 47–51 °C near-threshold (50 μm) 25-Hz stimulation of the RF_{center}. Solid line superimposed on data points between 5 and 10 s is best fitting linear regression line. X-intercept of regression equation = 8.8 s (i.e., full recovery of spontaneous/poststimulus RA neuron MFR to values matching those obtained prior to the exposure to 47–51 °C skin heating did not occur until 8.8 s after the exposure was terminated). Error bars are ±1 standard errors of the mean.

Amplitude-Dependence of the RA Neuron Response Modifications that Accompany 25-Hz Stimulation with a 47–51 °C Probe

The across-neuron distribution (for the 35 RA neurons in the sample; barplots on left in Fig. 5*A*) of the alterations of MFR and entrainment (R) reveals that when the 25-Hz stimulus to the RF_{center} was near-threshold (10–50 μm) and applied with a 47–51 °C probe, most RA neurons in the sample underwent a substantial suppression of both MFR and entrainment R (relative to the values of MFR and R obtained when the probe was maintained at a temperature between 25 and 38 °C). Both the suppression of MFR and R associated with 47–51 °C probe contact is highly significant: that is, average ΔMFR = –0.31, the 99% confidence interval extending from –0.46 to –0.16 and average ΔR = –0.39, the 99% confidence interval extending from –0.54 to –0.25.

In striking contrast, when the amplitude of the 25-Hz stimulus was suprathreshold (100–200 μm; barplots on left of Fig. 5*B*) and applied with the probe at 47–51 °C, relatively few of the RA neurons underwent a suppression of either MFR or R. Furthermore, comparison of the barplots on the left of Figure 5 reveal that in those relatively few instances when a suppression of RA neuron MFR and R did accompany suprathreshold (100–200 μm) 25-Hz stimulation at 47–51 °C (plots on left of Fig. 5*B*), the magnitude of the suppression was smaller than when the 25-Hz stimulus was near-threshold (10–50 μm; plots on left of Fig. 5*A*). Overall, the effect of 47–51 °C skin contact on RA neuron MFR and entrainment to suprathreshold stimuli was facilitatory, although this effect was not statistically significant. More specifically, average ΔMFR was +0.08, the 99% confidence interval extending from –0.09 to +0.24 and average ΔR was +0.04, the 99% confidence interval extending from –0.08 to +0.15. When evaluated using the paired T-test, the difference in the effect of 47–51 °C probe contact on the RA neuron response to near- versus suprathreshold 25-Hz stimulation of the RF_{center} was statistically significant for both MFR (P < 0.001) and entrainment (P < 0.05).

The RECOVERY trials following the noxious-heat TEST phase of the stimulation protocol (during which the stimuli were again applied with a 38 °C probe) confirm that suppression of RA neurons' responses to near-threshold stimuli during TEST trials is due specifically to the high probe temperature (see panels on right in Fig. 5). Thus, for the near-threshold RECOVERY trials, the average ΔMFR = 0.04 (±0.17 for the 99% confidence interval) and the average ΔR = –0.04 (±0.12 for the 99% confidence interval), which means that statistically the RECOVERY responses are not different from the CONTROL responses.

Effects of Intradermal Algogen Injection

Intradermal Injection of Capsaicin

The firing rate histogram in Figure 6*A* shows the "spontaneous" spike discharge activity of an area 3b RA neuron recorded in the absence of intentional mechanical skin stimulation before, during (at arrow labeled CAP), and for 23 min after the intradermal injection of capsaicin (CAP) at a skin site located ~8 mm from the neuron's RF_{center}. This RA neuron, like the other 8 RA neurons studied in the same way, exhibited 1) a large, but transient (persisting for ~15 s) increase in MFR after the injection (postinjection peak MFR is >4× the MFR recorded

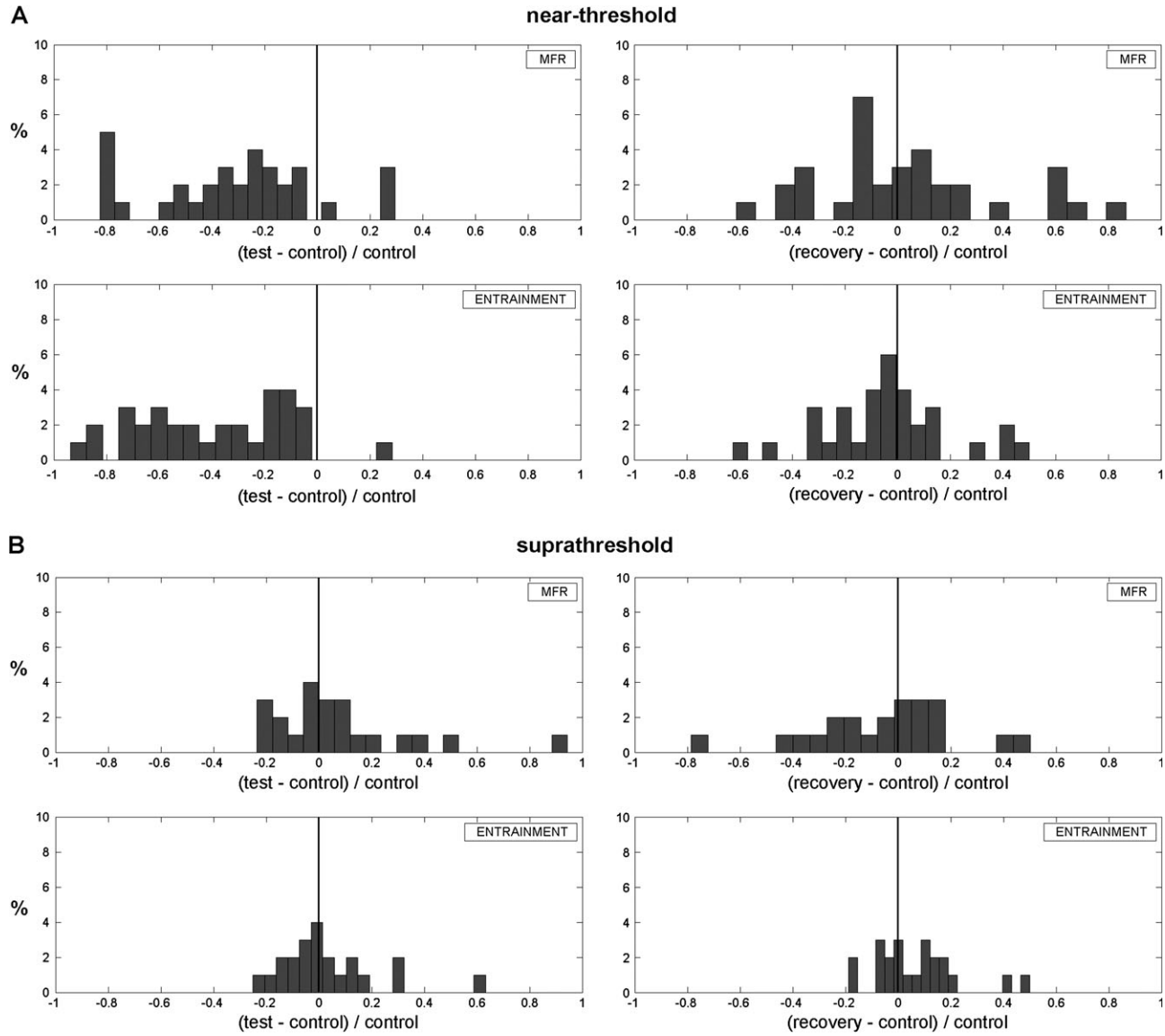

Figure 5. Effects of 47–51 °C contact on response of RA neurons to near-threshold versus suprathreshold stimulation of the RF_{center}. (*A*) Top left histogram: Distribution of the MFR alteration (ΔMFR) that accompanied near-threshold (10–50 μm) 25-Hz stimulation with the probe at 47–51 °C. ΔMFR was computed as the average MFR in TEST trials minus average MFR in CONTROL trials divided by the average MFR in CONTROL trials; that is, magnitude of the MFR alteration is expressed as a fraction of the CONTROL MFR. Negative/positive value of ΔMFR indicates that MFR decreased/increased in TEST trials; 0 indicates no change. Top right histogram: ΔMFR computed as average MFR in RECOVERY trials minus average MFR in CONTROL trials. Note that unlike the distribution of ΔMFR on the left, this distribution is centered on 0, indicating no difference between the average across-neuron MFR for the RECOVERY and CONTROL trials. Bottom left histogram: Distribution of the alteration of R (ΔR; computed using same approach as that used to obtain ΔMFR—see above) that accompanied near-threshold (10–50 μm) 25-Hz stimulation with the probe at 47–51 °C. Bottom right histogram: ΔR was computed as average R in RECOVERY trials divided by the average R in CONTROL trials. Unlike the distribution of ΔR shown at the left, in this case the distribution of ΔR is centered on 0 (indicating no difference between the average across-neuron R in the RECOVERY and CONTROL trials). All histograms computed from data obtained from the same 35 RA neurons. (*B*) Summary of MFR and R observations derived from 24 of the 35 RA neurons whose data are summarized in the histograms in A. Same format as in A. With one exception, stimulus conditions were the same as those used to obtain the data shown in A: that is, the amplitude of 25-Hz stimulation of the RF_{center} was suprathreshold (100–200 μm).

prior to the injection) and 2) a secondary, but relatively minor elevation of MFR at ~12–15 min after the injection.

Figure 6*B* shows the average magnitude and time course of the effect of intradermal capsaicin injection on RA neuron MFR in the absence of intentional mechanical skin stimulation. The dotted line shows normalized data obtained from 9 RA neurons—that is, maximal postinjection MFR for each neuron was set = 1.0, and MFR at all other time points is expressed as a fraction of that value. This plot not only confirms that intradermal capsaicin injection is followed by a rapid and vigorous increase of RA neuron activity but also, in addition, reveals that the initial period of increased spike firing that follows capsaicin injection wanes quickly (for the 9 RA neurons studied in this way the capsaicin-evoked increase of MFR recovered to ½ max at ~11 s after the injection). Moreover, a second, but much smaller elevation of above-background RA neuron spike firing occurs between 25 and 40 s after capsaicin injection (Fig. 6*B*), and for a prolonged (2–3h) period, the spike firing of RA neurons remains more irregular /"bursty" than it was before the injection (this latter feature of the RA neuron

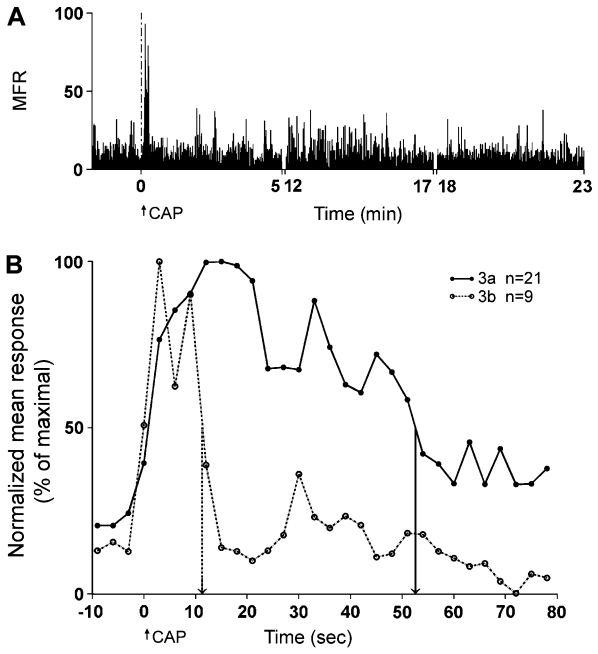

Figure 6. RA neuron response to intradermal injection of capsaicin (CAP). (*A*) Histogram showing MFR of exemplary area 3b RA neuron in the absence of mechanical skin stimulation before, during, and for 23 min following the intradermal injection of capsaicin. Note that: 1) the peak elevation of MFR associated with the injection develops within seconds and 2) MFR remains elevated for ~15 s after the injection. A subsequent, but relatively minor elevation of MFR occurred during the period between 12 and 15 min after the injection. (*B*) Comparison of normalized average area 3b RA neuron ($n = 9$) and area 3a nociresponsive neuron MFR ($n = 21$; from Whitsel, Favorov, Li, Quibrera, and Tommerdahl 2009) before and after intradermal capsaicin injection (at time 0). Downward arrow indicates time (for RA neurons at ~11 s after injection onset; for area 3a nociresponsive neurons at ~52 s after injection onset) at which the capsaicin-induced increase in MFR declined to half-maximal.

response to capsaicin was not evaluated quantitatively). In striking contrast to the capsaicin-evoked response of area 3b/1 RA neurons, nociresponsive area 3a neuron MFR (see the solid-line plot in Fig. 6*B*) increases more slowly, but progressively, subsequent to intradermal capsaicin injection and requires a much longer time (~52 s) to recover to ½ max (Whitsel, Favorov, Li, Quibrera, and Tommerdahl 2009).

Effects of 47–51 °C Skin Contact versus Intradermal Capsaicin Injection on RA Neurons

Figure 7 compares the effects of 49 °C probe contact ("heat"; histograms on the left) and intradermal capsaicin injection (histograms on the right) on the MFR response of a representative area 3b RA neuron to near-threshold (50 μm) 25-Hz stimulation of the RF_{center}. It is apparent that for this neuron both 49 °C probe contact with the RF_{center} and intradermal capsaicin (injected at a site 5 mm proximal to the stimulus site) resulted in a substantial suppression of the neuron's MFR response to the 25-Hz stimulus. The effects on near-threshold 25-Hz stimulation of the RF_{center} of 1) 47–51 °C probe contact and 2) intradermal algogen were compared for 3 other RA neurons that were studied in the same way as the neuron whose data are illustrated in Figure 7—for each of these neurons a substantial suppression of the MFR response to near-threshold 25-Hz stimulation of the RF_{center} resulted either from 47 to 51 °C probe contact with the RF_{center} or intradermal capsaicin injection.

Intradermal Injection of α β me ATP

Figure 8 shows results obtained from an area 1 RA neuron prior to and after intradermal injection of a different algogen (α β me ATP) at a site 7 mm from the RF_{center}. Like the approach used to study the effect of intradermal capsaicin on RA neurons (see Fig. 7), the effect of α β me ATP was determined 1) in the absence of intentional stimulation (firing rate histogram at top of Fig. 8) and 2) on the neuron's response to near-threshold (50 μm) stimulation of the RF_{center} (PST histograms at bottom). Like the effect of intradermal capsaicin injection, in the absence of intentional mechanical skin stimulation, injection of α β me ATP was followed not only by a brief and vigorous elevation of MFR (rate histogram at top) but also by a substantial suppression of the neuron's MFR response to near-threshold 25-Hz stimulation of the RF_{center} (see superimposed PST histograms—middle panel and ΔPST in bottom panel). Similar results were obtained from 3 other RA neurons studied in the same way (data not shown).

The Effect of Intradermal Capsaicin Injection on the RA Neuron MFR Response to 25-Hz Stimulation of the RF_{center} is Amplitude-Dependent

The PST histograms in Figure 9 show the MFR response of a representative area 3b RA neuron to 25 Hz near-threshold (25 μm; right column) versus suprathreshold (200 μm; left column) stimulation of the RF_{center} at successive 15-min intervals during the >75-min period subsequent to the intradermal injection of capsaicin (at time "0"). The injection was made at a site 10 mm proximal to the RF_{center}. These observations demonstrate that over the entire post-capsaicin period during which recordings of stimulus-evoked spike discharge activity were obtained, the MFR response of this RA neuron to near-threshold 25-Hz stimulation of the RF_{center} remained suppressed (relative to the precapsaicin MFR response to the same stimulus), whereas over the same time period this RA neuron's MFR response to suprathreshold 25-Hz stimulation of the same skin site (the RF_{center}) was enhanced (relative to the precapsaicin response to same-site 200 μm 25-Hz stimulation).

Figure 10 summarizes results obtained from 3 simultaneously recorded area 3b RA neurons (differentiated on the basis of spike amplitude). For each of these RA neurons, the MFR and entrained response to 25-Hz stimulation of the RF_{center} was determined (using the multiple amplitude stimulation protocol) before intradermal capsaicin injection (at time "0") and subsequently at successive 15-min intervals during the >75-min period following the injection at each of 3 different stimulus amplitudes—that is, 50 μm (left column), 100 μm (middle column), and 200 μm (right column). The plots in Figure 10 reveal that for each of these neurons, intradermal capsaicin injection was followed by: 1) a prolonged enhancement of both stimulus-evoked MFR and entrainment (~45 min for MFR; >75 min for R) when the amplitude of the 25-Hz stimulus was suprathreshold (100 or 200 μm; plots in middle and right panels) but 2) by a prolonged suppression of both stimulus-evoked MFR and R when stimulus amplitude was near-threshold (50 μm; plots in left panels). Comparable observations were obtained from 4 other RA neurons (2 area 3b neurons, 2 area 1 neurons —including the neuron that provided the data illustrated in Fig. 9).

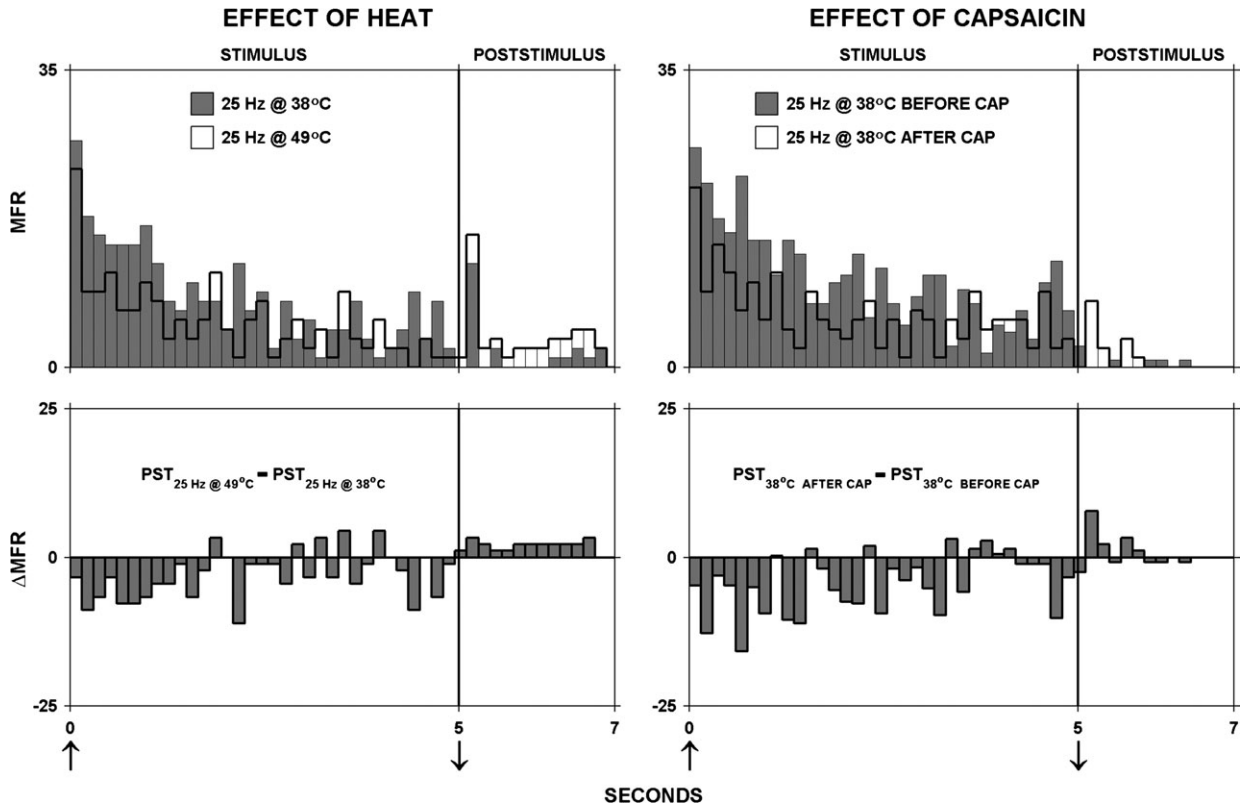

Figure 7. Comparison of the effect of heated skin contact versus capsaicin (CAP) on the same RA neuron. Panels at top: Superimposed PST histograms showing effects of 49 °C skin contact (top left) and intradermal capsaicin injection (top right). Panels at bottom: Difference PSTs for conditions described above. Arrows beneath abscissa indicate time of stimulus onset (↑; at time zero) and termination (↓; at 5 s after stimulus onset).

Discussion

Perceptual Implications of the Bipolar Effect of Skin Nociceptor Afferent Drive on SI RA Neuron MFR and Entrainment

The authors regard the suppression of the area 3b/1 RA neuron MFR response to near-threshold 25-Hz stimulation that accompanies contact of the RF_{center} with a 47–51 °C probe (Figs 2–5, 7) or follows intradermal algogen injection (Figs 7–10), as fully consistent with 1) the impairment by ongoing pain of the human capacity to detect a vibrotactile or punctate mechanical skin stimulus (Stevens et al. 1977; Apkarian et al. 1992, 1994; Hollins et al. 1996; Bolanowski et al. 2000, 2001) and 2) the reports (Hollins et al. 1996, 2001) that vibrotactile and pain sensitivities are inversely related in patients with temporomandibular pain but not in pain-free individuals.

The present study's observation that the polarity (–/+) of the effect of nociceptive afferent drive on the SI RA neuron MFR response to 25-Hz stimulation of the RF depends on stimulus amplitude (see Figs 2–3,5,9–10) enables cortical-level neuromechanistic explanation of the reports of hyperesthesia in human subjects experiencing clinical or experimentally induced pain (Eliav and Gracely 1998; Svensson et al. 1998; Ayesh et al. 2007). That is, hypoesthesia in the presence of pain/nociceptor afferent drive might be associated with weak/near-threshold mechanical skin stimulation because under this condition, the contralateral SI RA neuron MFR response to a tactile stimulus is smaller than normal; whereas hyperesthesia in the presence of strong pain/nociceptor afferent drive might be associated with stronger/suprathreshold mechanical skin stimulation because under this condition, the stimulus-evoked RA neuron MFR response in the contralateral SI is larger than normal.

Consistent with the present study's observation that the nociceptive afferent drive which accompanies noxious skin heating or intradermal algogen injection degrades SI RA neuron entrainment to near-threshold 25-Hz stimulation of the RF_{center} are 1) published reports showing that the human perceptual capacity to discriminate frequency of low-amplitude/near-threshold vibrotactile stimulation is subnormal in the presence of experimental or clinical pain (Hollins et al. 1996; Hollins and Sigurdsson 1998) and 2) pioneering studies which not only revealed that the mechanoresponsive RA neurons of areas 3b/1 utilize a spike firing periodicity code to signal/encode frequency of sinusoidal vertical skin displacement stimulation (Mountcastle et al. 1969, 1990; Mountcastle 1984) but also demonstrated that destruction of areas 3b/1 in the contralateral SI cortex eliminates the ability to discriminate frequency of vibrotactile stimulation at frequencies between 10 and 50 Hz (LaMotte and Mountcastle 1979).

Unlike the clear parallel between the suppressive effects of skin nociceptor afferent drive on the SI RA neuron MFR response and human perceptual sensitivity to weak/near-threshold mechanical skin stimulation, there is no clear parallel in the published psychophysical literature for the present study's finding that in the presence of nociceptor afferent drive SI RA neuron entrainment to suprathreshold 25-Hz stimulation of the RF_{center} is normal/near-normal or, not infrequently, is

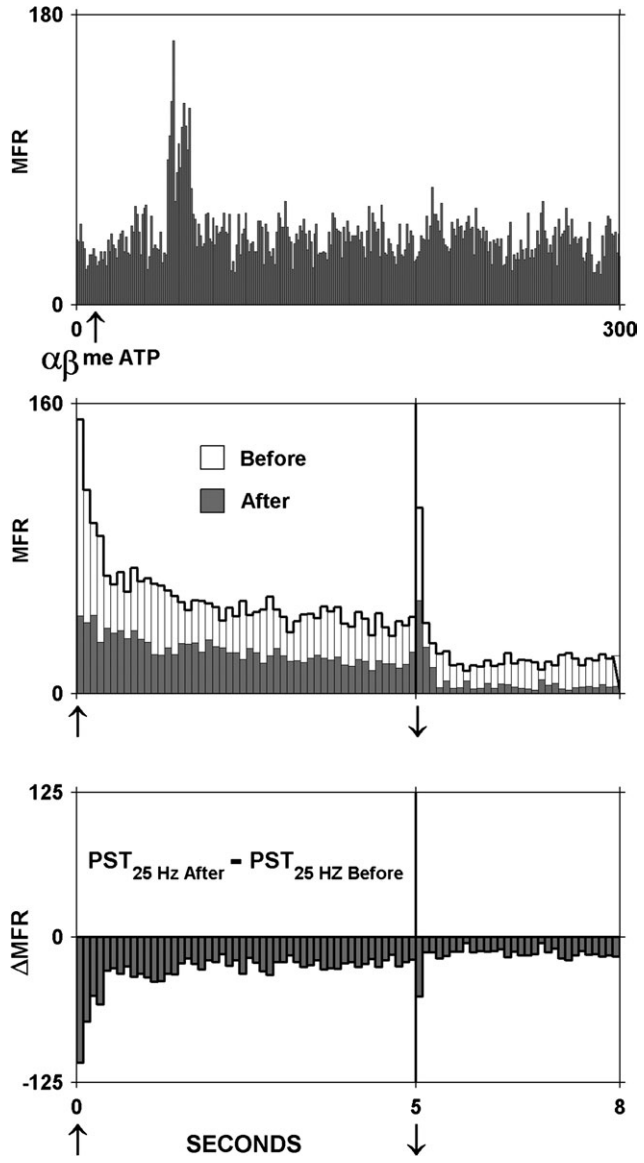

Figure 8. The effects on an exemplary RA neuron of intradermal α β methylene ATP. Top: MFR versus time histogram showing effect of intradermal injection of α β me ATP (time of injection indicated by ↑). Middle: Superimposed PST histograms showing the same RA neuron's MFR response to 25-Hz stimulation before and after the injection of α β me ATP. Arrows beneath the abscissa indicate the time of onset (↑; at time 0) and termination (↓ at 5 s after stimulus onset) of 25-Hz stimulation. Bottom: Difference PST histogram for the same RA neuron showing suppressive effect of α β me ATP injection. Format same as above.

significantly enhanced/improved. Because it is established (Mountcastle et al. 1969, 1990; for review see Mountcastle 1984, 1998) that the ability of RA neurons in the contralateral hemisphere to entrain to 10–50 Hz skin flutter stimulation underlies the perceptual ability to discriminate such stimuli solely on the basis of frequency, the prominent amplitude-dependency of the effect of skin nociceptor afferent drive on RA neurons (illustrated in Figs 2–3,5,10) leads the authors to anticipate that future studies of the capacity of humans to discriminate skin flutter stimuli which differ only in frequency will find that whenever the stimuli used in such investigations are 1) suprathreshold and 2) applied in the presence of pain/nociceptive afferent drive, a subject's frequency discriminative capacity is either little affected or enhanced (relative to the significant pain-induced alteration/decrease of the ability to discriminate the frequency of near-threshold skin flutter stimulation; Hollins and Sigurdsson 1998; Hollins et al. 2001).

Why haven't published studies of the effect of pain/nociceptor afferent drive on human vibrotactile frequency discriminative capacity detected bipolar amplitude-dependent alterations consistent with the RA neuron observations obtained in the present study? Although the answer to this question may be more complex, one possibility is that this situation exists because, at least to date, the impact of pain/nociceptor afferent drive on human vibrotactile frequency discriminative capacity has been studied using near-threshold amplitudes of skin flutter stimulation (Hollins and Sigurdsson 1998; Hollins et al. 2001). The evidence obtained in the experiments of the present study suggests that while the exclusive use of near-threshold skin flutter stimulation ensures that maximal estimates of the suppressive effect of pain/nociceptor afferent drive on frequency discriminative capacity are obtained, this approach is incapable of providing evidence bearing on the possibility (suggested by the RA neuron observations obtained in the present study) that the perceptual capacity to discriminate suprathreshold flutter stimuli solely on the basis of frequency either is little affected (relative to the significant and substantial reduction that occurs when the stimulus is near-threshold) or is significantly enhanced in the presence of pain/nociceptor afferent drive.

Mechanisms Underlying the Bipolar (–/+) Effect of Nociceptor Afferent Drive on SI RA Neuron MFR and Entrainment to Skin Flutter Stimulation

Prior studies have shown that the RA-I skin afferents (the major source of A_β skin mechanoreceptor input to SI RA neurons; Mountcastle 1984, 1998) are unaffected/insensitive to either intradermal algogen injection or elevations of skin temperature to values between 38 and 49 °C (e.g., Szolcsanyi 1987; LaMotte et al. 1992; Torebjork et al. 1992). It seems evident, therefore, that alterations of the stimulus-evoked response of CNS neurons at one or more levels of the projection path that conveys stimulus-evoked input to SI cortex must be responsible for the stimulus-intensity dependent, bipolar modification of stimulus-evoked SI RA neuron MFR and entrainment that accompanies heat- or algogen-evoked skin nociceptor afferent drive.

The findings obtained in the present study provide no information about either the site(s) or nature of the cellular-level mechanisms responsible for the activity/stimulus-dependent bipolar alteration of RA neuron MFR and entrainment that accompanies skin nociceptor afferent drive. Nevertheless, observations reported recently by others lead the authors to propose that the bipolar stimulus-dependent alterations of RA neuron MFR and entrainment that accompany nociceptor afferent drive revealed by the experiments of the present study are outcomes of an activity-dependent action of the neurotransmitter γ-aminobutyric acid (GABA) on the $GABA_A$ receptors of SI RA neurons. Especially meaningful in this regard is the recent, but already considerable, evidence that indicates that even in adult subjects "the alteration of cortical neuron membrane ion conductance which accompanies GABA binding to $GABA_A$ receptors is not fixed, but is prominently activity-dependent." For example, even a relatively brief (≥5 s)

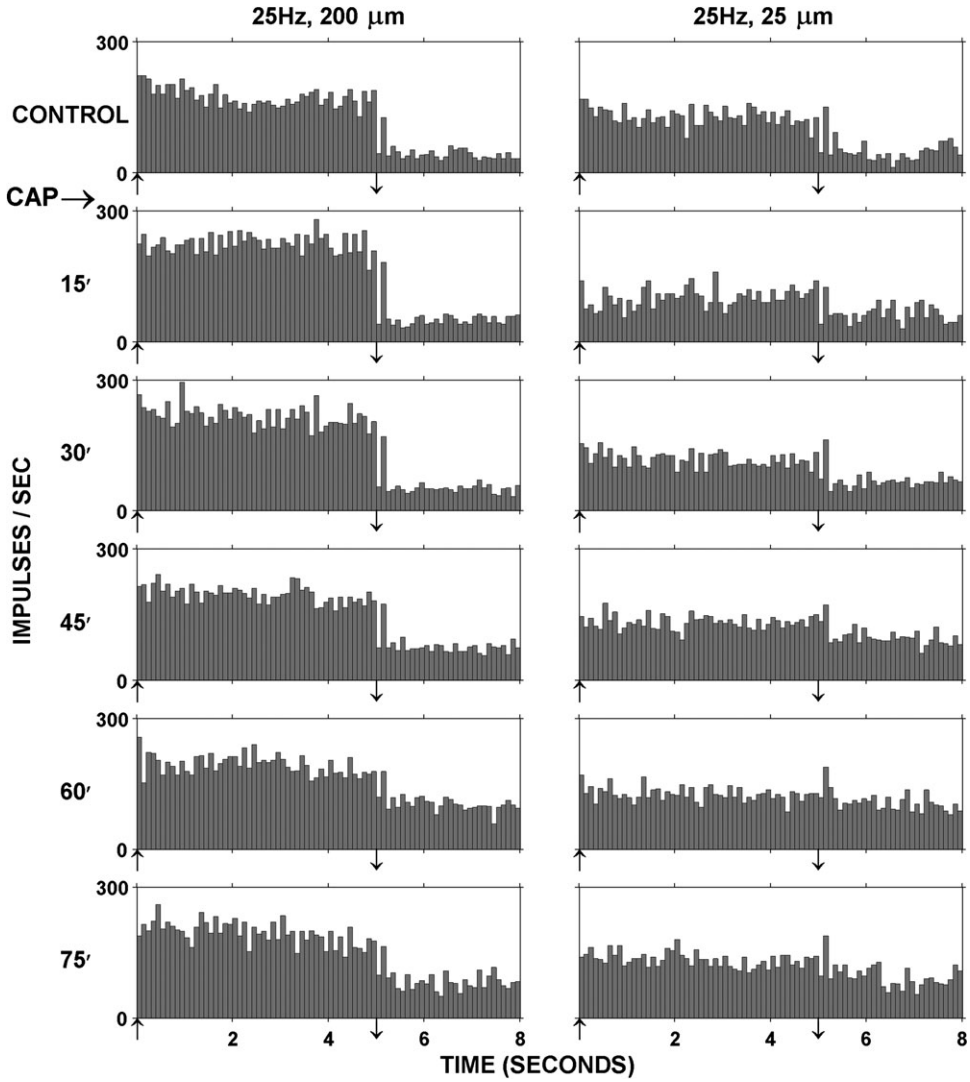

Figure 9. Amplitude-dependence of capsaicin effect on RA neuron MFR. PSTs histograms showing exemplary area 3b RA neuron's MFR response to 5 s suprathreshold (200 μm; left column) versus near-threshold (25 μm; right column) 25-Hz flutter stimulation of the RF_{center} before ("Control" PSTs shown at top), and at successive 15-min intervals after the intradermal injection of 50 μL of 1% capsaicin (injection was at time "0"). Note that when the amplitude of 25-Hz stimulation was suprathreshold, the stimulus-evoked MFR remained elevated (relative to the precapsaicin values obtained under the same stimulus conditions) for >75 min after the injection of capsaicin. In contrast, throughout the same postinjection period the MFR values associated with near-threshold skin flutter stimulation were suppressed (relative to the precapsaicin values obtained under the same stimulus conditions).

exposure to conditioning excitatory afferent drive converts the action of GABA on cortical pyramidal neuron $GABA_A$ receptors from inhibitory/hyperpolarizing to excitatory/depolarizing (layer II-II pyramidal neurons in sensorimotor cortex—Lee et al. 2009; hippocampal pyramidal neurons—Staley et al. 1995; Kaila et al. 1997; Gulledge and Stuart 2003; Isomura et al. 2003; Stein and Nicoll 2003; Walters 2004; Szabadics et al. 2006; Fujiwara-Tsukamoto et al. 2007; pyramidal neurons in temporal neocortex—Kaneda et al. 2005; for in-depth discussion of the cellular/biophysical mechanisms underlying the bipolar action of GABA on neuronal $GABA_A$ receptors see Staley and Proctor 1995, 1999; Taira et al. 1997; Voipio and Kaila 2000; Gulledge and Stuart 2003; Fujii et al. 2004; Fiumelli et al. 2005; Morita et al. 2006; Khirug et al. 2008; Bannai et al. 2009; for overview of the excitatory effects of GABA and their putative functional meaning see Marty and Llano 2005).

Guided by the above-described recent evidence, the authors consider it as plausible, if not likely, that: "1) the action of GABA on SI RA neurons is different at different levels of stimulus-evoked RA neuron spike firing (i.e., activity-dependent) and 2) such an activity-dependence of the action of GABA on SI RA neurons accounts for the present study's observation that the effect of nociceptive afferent drive on the MFR and entrained responses of RA neurons to 25-Hz stimulation of the RF_{center} changes progressively from suppressive/inhibitory to augmenting/excitatory as stimulus amplitude/intensity is increased from near-threshold to suprathreshold values."

Figure 11 shows the CNS structures (sensory projection pathways, interareal corticortical connections, cell types, and cellular-level mechanisms) hypothesized by the authors to be responsible not only for the release of GABA in areas 3b/1 of SI cortex in response to skin nociceptor afferent drive but also for a bipolar (–/+) and activity-dependent GABA action on SI RA neurons (mediated via postsynaptic $GABA_A$ receptors). The principal elements of our hypothesis—currently under evaluation using both in vivo (Whitsel, Favorov, Li, Lee, and

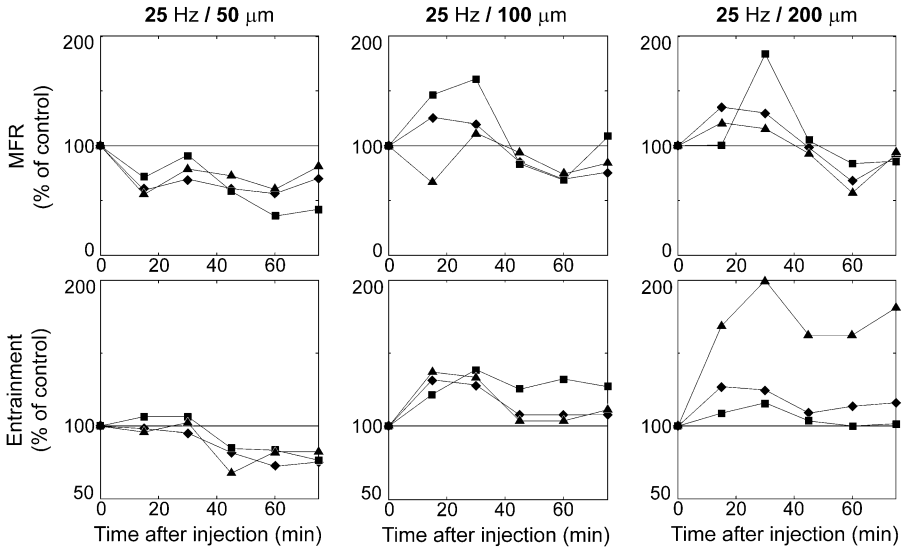

Figure 10. Amplitude-dependence and bipolarity of effect of capsaicin on RA neuron MFR and entrainment. Top panels: Each panel (left, middle, right) shows the effect of intradermal capsaicin on the normalized MFR response (MFR was corrected for spontaneous activity: i.e., $MFR_{STIM} - MFR_{NOSTIM}$; expressed as % of the control/precapsaicin MFR) of 3 simultaneously recorded area 3b RA neurons to the indicated amplitude (50 μm—panel on left, 100 μm—middle panel, 200 μm—right panel) of 25-Hz stimulation of the RF_{center}. Data points for the same neuron are indicated by the same symbol. Bottom panels: Each panel shows the effect of intradermal capsaicin on entrainment (expressed as % of the precapsaicin entrainment value) for the same 3 RA neurons whose MFR data are summarized in the panels at the top. Same correspondence between symbols and neurons as in top panels.

Tommerdahl 2009) and in vitro (Lee et al. 2009) approaches—are as follows: 1) area 3a nociresponsive pyramidal neurons vigorously activated by either 47–51 °C skin contact or intradermal algogen injection (Whitsel, Favorov, Li, Quibrera, and Tommerdahl 2009) release GABA in areas 3b/1 (not only from the spatially extensive and strongly interconnected—via gap junctions—network of GABAergic interneurons activated by glutamate (GLU) release from the terminals of cortico-cortical axons arising in the nociresponsive regions of area 3a—Burton and Fabri 1995; Fukuda et al. 2006; Whitsel, Favorov, Li, Quibrera, and Tommerdahl 2009 but also from neurons and glia in the region of areas 3b/1 in which a substantial increase in $[K^+]_o^+$ occurs reliably in response to peripheral afferent drive—Koch and Magnusson 2009) and 2) the GABA released in the area 3b/1 cell column(s) whose neurons have an RF_{center} corresponding to the skin site contacted by the 25-Hz skin stimulus leads to hyperpolarization/inhibition when RA neuron MFR is low (as during near-threshold 25-Hz stimulation of the RF_{center}) but is depolarizing/excitatory when RA neuron MFR is high (as it is during suprathreshold 25-Hz stimulation of the RF_{center}).

Although experimental identification of the cellular mechanisms which enable conversion of GABA's effect on SI RA neurons from hyperpolarizing/inhibitory to depolarizing/excitatory is at a relatively early stage (Lee et al. 2009; Whitsel, Favorov, Li, Lee, and Tommerdahl 2009), the evidence obtained to date is consistent with the idea that 1) the responsible mechanisms are triggered into action by a co-occurrence of strong direct thalamocortical afferent drive and GABA binding to $GABA_A$ receptors and 2) the end-result is a substantial increase of intracellular chloride ($[Cl^-]_i$) in the affected RA neurons. Although the full spectrum of cellular-level events and the relative contribution of each to the increase of $[Cl^-]_i$ proposed to occur in RA neurons in response to a co-occurrence of strong direct thalamocortical afferent drive and GABA binding to $GABA_A$ receptors remains uncertain, it is presumed that, as has been established for hippocampal pyramidal neurons, the most significant events include: 1) preservation of the normal transmembrane HCO_3^- gradient due to HCO_3^-/CO_2 redistribution; 2) continued operation of a still uncharacterized Cl^- uptake mechanism located in the somal region of the neuron (a bicarbonate-dependent mechanism has been suggested; Khirug et al. 2008); and 3) extracellular K^+ accumulation (at least, in part, due to K^+ release from neighboring glia) which, if sufficiently large, stops and even reverses Cl^- extrusion by membrane ion transporters (Fujiwara-Tsukamoto et al. 2007). Because an increase of $[Cl^-]_i$ would shift the reversal potential (E_{GABA}) of RA neurons toward more depolarized values, GABA's action in the presence of an increasingly elevated $[Cl^-]_i$ is anticipated to be accompanied by a progressively smaller hyperpolarization/inhibition of the RA neuron response to the GLU released by the thalamocortical afferent drive evoked by stimulation of the RF_{center}. Furthermore, when an RA neuron's $[Cl^-]_i$ is elevated sufficiently due to the co-occurrence of strong direct thalamocortical afferent drive, generated by a suprathreshold mechanical stimulus to the RF_{center}, and GABA binding to $GABA_A$ receptors, both the action of GABA as well as the GLU released from the terminals of thalamocortical afferents would become depolarizing. The end result is that under this condition (high RA neuron $[Cl^-]_i$ and suprathreshold mechanical stimulation of the RF_{center}) both GLU and GABA would contribute to increased RA neuron spike firing because the values of both E_{GABA} and E_{GLU} of the affected neurons are more depolarized than the threshold for neuronal spike firing.

Although the mechanisms illustrated in Figure 11 appear to satisfactorily account for the bipolar and activity-dependent alterations of RA neuron MFR and entrainment that accompany algogen injection or noxious skin heating, they do not explain the brief (~10 s) and relatively weak increase of RA neuron spiking firing that reliably follows intradermal capsaicin injection—relative to the more prolonged (~50 s; Fig. 6*B*)

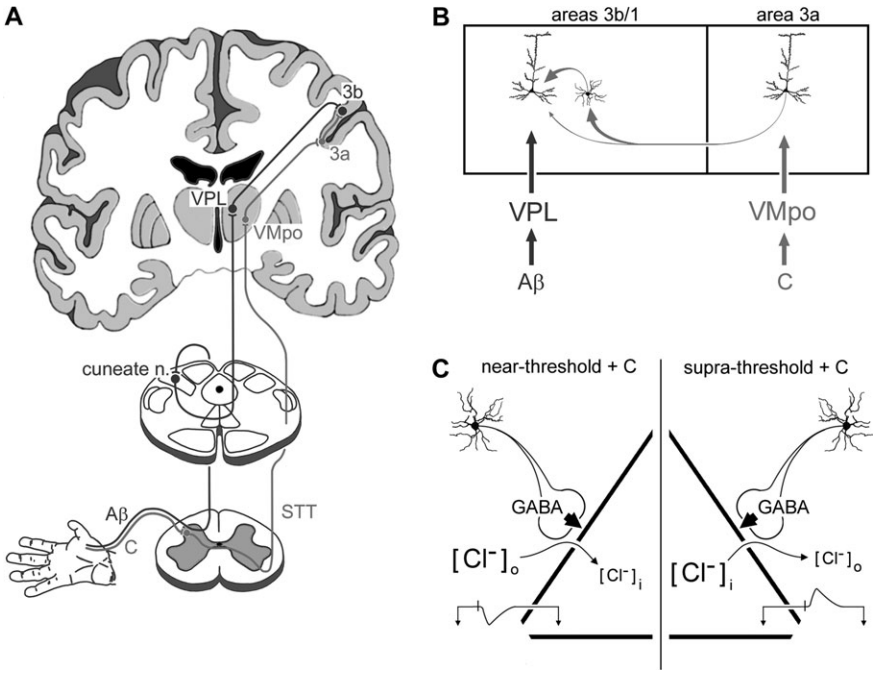

Figure 11. Neuromechanistic interpretation of the activity-dependent, bipolar SI RA neuron response alteration that accompanies skin nociceptor afferent drive. (*A*) Neuroanatomical projection paths that convey stimulus-evoked activity originating in: 1) skin C-nociceptors to nociresponsive pyramidal neurons in the contralateral area 3a (Craig 2003, 2006; Craig and Blomqvist 2002; Whitsel, Favorov, Li, Quibrera, and Tommerdahl 2009) and 2) RA-I skin mechanoreceptors to RA neurons in contralateral areas 3b/1 (Mountcastle et al. 1969, 1990; Mountcastle 1984, 1998; LaMotte and Mountcastle 1975, 1979). (*B*) Schematic diagram showing: 1) thalamocortical projections (vertical arrows) that convey activity from the thalamic region activated by A_β skin mechanoreceptor afferent drive (nucleus ventralis posterolateralis, VPL) to areas 3b/1; and from the region activated by C-nociceptor afferent drive (VMpo) to area 3a; and 2) corticocortical connections (arrow originating in area 3a) that, when active, trigger the excitation of GABAergic interneurons in areas 3b/1. (*C*) Area 3b/1 RA neuron (triangle) showing hypothesized transmembrane distribution of Cl^- and the synaptic effect of GABA on RA neuron $GABA_A$ receptors under the 2 conditions evaluated in the experiments described in this paper: on the left—GABA triggers RA neuron membrane hyperpolarization/neuronal inhibition when the direction of Cl^- diffusion through activated $GABA_A$ channels is inward (as it is when the RA neuron's activity is low); on the right—GABA leads to membrane depolarization/neuronal excitation when the direction of Cl^- diffusion through activated $GABA_A$ channels is outward (as it is when the RA's neuron's activity is high).

and vigorous activation of nociresponsive area 3a neurons (Whitsel, Favorov, Li, Quibrera, and Tommerdahl 2009) and C-nociceptor afferents (LaMotte et al. 1992) triggered by capsaicin injection. Because no comparable response is observed when an equal volume of saline is injected intradermally at a site located 4–10 mm from the RF_{center}, the authors do not regard the increased RA neuron MFR that follows algogen injection as attributable to a transient mechanical event associated with the injection. Instead, it seems possible (but unproven) that this may reflect the activation by capsaicin of cutaneous afferent fibers other than those that supply C-nociceptors (e.g., A_δ skin nociceptive afferents and/or the C-fibers that supply skin mechanoreceptors—afferents that have been reported by others to respond weakly and unreliably to capsaicin (Foster and Ramage 1981; Kenins 1982; Szolcsanyi 1987; LaMotte et al. 1992).

On the Modality Specificity of SI Neurons

The authors view the observations obtained in the present study to conflict fundamentally with the widely held view that the information encoded by the different classes (modalities) of peripheral receptors that exist in the skin of humans and nonhuman primates are kept isolated/separate until a stage of CNS processing later/higher than areas 3b and 1 of primary somatosensory cortex (Sur et al. 1984; Mountcastle 1998; also for discussion of role of GABA see Dykes et al. 1984, and Alloway and Burton 1991). Instead, the results demonstrate that 1) the RA neurons in areas 3b and 1, in addition to processing low-threshold skin mechanoreceptor input, are the recipients of significant influences that originate in skin nociceptors and 2) skin nociceptor activity can lead to substantial modification of the SI RA neuron response to vibrotactile stimulation. Because of the strong parallels between the effects of pain/skin nociceptor afferent drive on 1) SI RA neurons and 2) the abilities of humans to detect and discriminate vibrotactile stimuli, the authors regard it as likely that the effects of experimental or clinical pain on human vibrotactile perception are attributable in part, if not entirely, to the effects of nociceptor afferent drive on SI RA neuron MFR and entrainment.

Because the evidence presented in this paper is indirect, it would be premature to conclude that the modulation by skin nociceptor afferent drive of the area 3b/1 RA neuron response to skin flutter is due solely to a corticocortical influence arising from nociresponsive neurons within area 3a. Nevertheless, consideration of the extensive corticocortical connections which link the 4 cytoarchitectonic areas that comprise anterior parietal cortex (Burton and Fabri 1995) not only makes across-modal modulatory influences of the type detected in the present study plausible (see Fig. 11) but also raises the possibility that such influences may contribute importantly to both normal and abnormal somesthetic perception.

Funding

National Institutes of Health RO1 grant (NS37501 to B.L.W.).

Notes

The authors thank Betsy Houston and Calvin Wong for expert technical assistance. *Conflict of Interest*: None declared.

References

Alloway KD, Burton H. 1991. Differential effects of GABA and bicuculline on rapidly- and slowly-adapting neurons in primary somatosensory cortex of primates. Exp Brain Res. 85:598–610.

Apkarian AV, Gelnar PA, Krauss BR, Szeverenyi NM. 2000. Cortical responses to thermal pain depend on stimulus size: a functional MRI study. J Neurophysiol. 83:3113–3122.

Apkarian AV, Stea RA, Bolanowski SJ. 1994. Heat-induced pain diminishes vibrotactile perception: a touch gate. Somatosens Mot Res. 11:259–267.

Apkarian AV, Stea RA, Manglos SH, Szeverenyi NM, King RB, Thomas FD. 1992. Persistent pain inhibits contralateral somatosensory cortical activity in humans. Neurosci Lett. 140:141–147.

Ayesh EE, Jensen TS, Svensson P. 2007. Hypersensitivity to mechanical and intra-articular electrical stimuli in persons with painful temporomandibular joints. J Dent Res. 86:1187–1192.

Bannai H, Levi S, Schweitzer C, Inoue T, Launey T, Racine V, Siperita J-B, Mikoshita K, Triller A. 2009. Activity-dependent tuning of inhibitory neurotransmission based on $GABA_AR$ diffusion dynamics. Neuron. 62:670–682.

Baron R, Baron Y, Disbrow E, Roberts TPL. 1999. Brain processing of capsaicin-induced secondary hyperalgesia—a functional MRI study. Neurology. 53:548–557.

Baron R, Baron Y, Disbrow E, Roberts TPL. 2000. Activation of the somatosensory cortex during Aβ-fiber mediated hyperalgesia. A MSI study. Brain Res. 871:75–82.

Bensmaia SJ, Craig JC, Johnson KO. 2006. Temporal factors in tactile spatial acuity: evidence for RA interference in fine spatial processing. J Neurophysiol. 95:1783–1791.

Bolanowski SJ. 1996. Tactile channels and their interactions. In: Franzen O, Johansson R, Terenius L, editors. Somesthesis and the neurobiology of the somatosensory cortex. Basel (Switzerland): Birkhauser Verlag. p. 103–108.

Bolanowski SJ, Gescheider GA, Fontana AM, Niemiec JL, Tromblay JL. 2001. The effects of heat-induced pain on the detectability, discriminability, and sensation magnitude of vibrotactile stimuli. Somatosens Mot Res. 18:5–9.

Bolanowski SJ, Maxfield LM, Gescheider GA, Apkarian AV. 2000. The effects of stimulus location on the gating of touch by heat- and cold-induced pain. Somatosens Mot Res. 17:195–204.

Burton H, Fabri M. 1995. Ipsilateral intracortical connections of physiologically defined cutaneous representations in areas 3b and 1 of macaque monkeys: projections in the vicinity of the central sulcus. J Comp Neurol. 355:508–538.

Craig AD. 2003. Pain mechanisms: labelled lines versus convergence in central processing. Ann Rev Neurosci. 26:1–30.

Craig AD. 2006. Retrograde analysis of spinothalamic projections in the macaque monkey: input to ventral posterior nuclei. J Comp Neurol. 499:965–978.

Craig AD, Blomqvist A. 2002. Is there a specific lamina I spinothalamocortical pathway for pain and temperature sensation? J Pain. 3:95–101.

Dykes RW, Landry P, Metherate R, Hicks TYP. 1984. Functional role of GABA in cat primary somatosensory cortex: shaping receptive fields of cortical neurons. J Neurophysiol. 52:1066–1093.

Eliav E, Gracely RH. 1998. Sensory changes in the territory of the lingual and inferior alveolar nerves following lower third molar extraction. Pain. 77:191–199.

Fiumelli H, Cancedda L, Poo M. 2005. Modulation of GABAergic transmission by activity via postsynaptic Ca^{++}-dependent regulation of KCC2 function. Neuron. 48:773–786.

Foster RW, Ramage AG. 1981. The action of some chemical irritants on somatosensory receptors of the cat. Neuropharm. 20:191–198.

Fujii H, Aihara K, Tsuda I. 2004. Functional relevance of "excitatory" GABA actions in cortical interneurons: a dynamical systems approach. J Integr Neurosci. 3:183–205.

Fujiwara-Tsukamoto Y, Isomura Y, Imanishi M, Fukai T, Takada M. 2007. Distinct types of GABA actions in pyramidal cells and interneurons during electrical induction of hippocampal seizure-like network activity. Eur J Neurosci. 25:2713–2725.

Fukuda T, Kosaka T, Singer W, Galuske RAW. 2006. Gap junctions among dendrites of cortical GABAergic neurons establish a dense and widespread intercolumnar network. J Neurosci. 26: 3434–3443.

Gulledge AT, Stuart GJ. 2003. Excitatory actions of GABA in the cortex. Neuron. 37:299–309.

Hamilton SG, McMahon SB, Lewin GR. 2001. Selective activation of nociceptors by P2X receptor agonists in normal and inflamed rat skin. J Physiol. 534:437–445.

Hamilton SG, Wade A, McMahon SB. 1999. The effects of inflammatory mediators on nociceptive behavior induced by ATP analogues in the rat. Brit J Pharm. 126:326–332.

Hamilton SG, Warburton J, Bhattacharjee A, Ward J, MacMahon SB. 2000. ATP in human skin elicits a dose related pain response which is potentiated under conditions of hyperalgesia. Brain. 123:1238–1246.

Hernandez A, Zainos A, Romo R. 2000. Neuronal correlates of sensory discrimination in the somatosensory cortex. Proc Natl Acad Sci U S A. 97:6191–6196.

Hollins M, Sigurdsson A. 1998. Vibrotactile amplitude and frequency discrimination in temporomandibular disorders. Pain. 75:59–67.

Hollins M, Sigurdsson A, Fillingim L, Goble AK. 1996. Vibrotactile threshold is elevated in temporomandibular disorders. Pain. 67:89–96.

Hollins M, Sigurdsson A, Morris KA. 2001. Local vibrotactile and pain sensitivities are negatively related in temporomandibular disorders. J Pain. 2:46–56.

Iadarola MJ, Berman KF, Zeffiro TA, Byas-Smith MG, Gracely RH, Max MB, Bennett GJ. 1998. Neural activation during acute capsaicin-evoked pain and allodynia assessed with PET. Brain. 121:931–947.

Isomura Y, Sugimoto M, Fujiwara-Tsukamoto Y, Yamamoto-Muraki S, Yamada J, Fukada A. 2003. Synaptically activated Cl- accumulation responsible for depolarizing GABAergic responses in mature hippocampal neurons. J Neurophys. 90:2752–2756.

Jones EG, Porter R. 1980. What is area 3a? Brain Res. 203:1–43.

Kaila K, Lamsa K, Smirnov S, Tara T, Voipio J. 1997. Long-lasting GABA-mediated depolarization evoked by high-frequency stimulation in pyramidal neurons of rat hippocampal slice is attributable to a network-driven, bicarbonate-dependent K+ transport. J Neurosci. 17:7662–7672.

Kaneda K, Fujiwara-Tsukamoto Y, Isomura Y, Takada M. 2005. Region-specific modulation of electrically induced synchronous oscillations in the rat hippocampus and cerebral cortex. Neurosci Res. 52: 83–94.

Kenins P. 1982. Responses of single nerve fibers to capsaicin applied to the skin. Neurosci Lett. 29:83–88.

Khirug S, Yamada J, Afzalov R, Voipio J, Khiroug L, Kaila K. 2008. GABAergic depolarization of the axon initial segment in cortical principal neurons is caused by the Na-K-2Cl cotransporter NKCC1. J Neurosci. 28:4635–4639.

Koch U, Magnusson AK. 2009. Unconventional GABA release: mechanisms and functions. Curr Opin Neurobiol. 19:305–310.

LaMotte RH, Lundberg LER, Torebjork HE. 1992. Pain, hyperalgesia and activity in nociceptive C units in humans after intradermal injection of capsaicin. J Physiol. 448:749–764.

LaMotte RH, Mountcastle VB. 1975. Capacities of humans and monkeys to discriminate between vibratory stimuli of different frequency and amplitude: a correlation between neural events and psychophysical measurements. J Neurophysiol. 38:539–559.

LaMotte RH, Mountcastle VB. 1979. Disorders in somesthesis following lesions of parietal lobe. J Neurophysiol. 42:400–419.

Lee J, Favorov OV, Tommerdahl M, Whitsel BL. 2009. Activity-dependent bipolar actions of GABA on sensorimotor cortical pyramidal neurons. Neurosci Abstr. 35:324.

Li Y, Kelly EF, Tommerdahl M, Metz CB, Whitsel BL. 2002. Modification by noxious skin heating of SI RA neuron dynamics. Neurosci Abstr. 28.

Li Y, Tommerdahl M, Whitsel BL. 2001. The SI response to vibrotactile stimulation modifies during noxious skin heating. Neurosci Abstr. 27.
Maihofner C, Forster C, Birklein F, Neuendorfer B, Handwerker HO. 2005. Brain processing during mechanical hyperalgesia in complex regional pain syndrome: a functional MRI study. Pain. 114:93–103.
Maihofner C, Schmelz M, Forster C, Neundorfer B, Handwerker HO. 2004. Neural activation during experimental allodynia: a functional magnetic resonance imaging study. Eur J Neurosci. 19:3211–3218.
Marty A, Llano I. 2005. Excitatory effects of GABA in established brain networks. Trends Neurosci. 28:284–289.
Maxfield LM, Bolanowski SJ. 1994. Vibrotactile thresholds under thermal pain: spatial factors and temperature effects. Psychonomic Soc. 35:33.
Maxfield LM, Bolanowski SJ. 1995. Coincident or dermatomal thermally induced pain affects vibrotactile sensitivity. Neurosci Abstr. 21:1636.
Morita K, Tsumoto K, Aihara K. 2006. Bidirectional modulation of neuronal responses by depolarizing GABAergic inputs. Biophys J. 90:1925–1938.
Mountcastle VB. 1984. Central nervous mechanisms in mechanoreceptive sensibility. Handbook of Physiology. In: Darian-Smith I, Brookhart JM, Mountcastle VB, editors. Section I: the nervous system III: sensory processes. Bethesda (MD): American Physiological Society. p. 789–878.
Mountcastle VB. 1998. The columnar organization of the neocortex. "perceptual neuroscience—the cerebral cortex", chapter 7. Cambridge (MA): Harvard University Press. p. 163–203.
Mountcastle VB, Steinmetz MA, Romo R. 1990. Frequency discrimination in the sense of flutter: psychophysical measurements correlated with postcentral events in behaving monkeys. J Neurosci. 10:3032–3044.
Mountcastle VB, Talbot WH, Sakata H, Hyvarinen J. 1969. Cortical neuronal mechanisms in flutter vibration studied in unanesthetized monkeys. Neuronal periodicity and frequency discrimination. J Neurophysiol. 32:452–484.
Peyron R, Schneider F, Faillenot I, Convers P, Barral F-G, Garcia-Larrea L, Laurent B. 2004. An fMRI study of cortical representation of mechanical allodynia in patients with neuropathic pain. Neurology. 63:1838–1846.
Ploner M, Pollock B, Schnitzler A. 2004. Pain facilitates tactile processing in human somatosensory cortices. J Neurophysiol. 92:1825–1829.
Powell TP, Mountcastle VB. 1959. The cytoarchitecture of the postcentral gyrus of the monkey Macaca mulatta. Bull Johns Hopkins Hosp. 105:108–131.
Rosso T, Aglioti SM, Zanette G, Ischia S, Finco G, Farina S, Fiaschi A, Tinazzi M. 2003. Functional plasticity in the human primary somatosensory cortex following acute lesion of the anterior lateral spinal cord: neurophysiological evidence of short-term cross-modal plasticity. Pain. 101:107–127.
Staley KJ, Proctor WR. 1999. Modulation of mammalian dendritic $GABA_A$ receptor function by the kinetics of Cl^- and HCO_3^- transport. J Physiol. 519:693–712.
Staley KJ, Soldo BL, Proctor WR. 1995. Ionic mechanisms of neuronal excitation by inhibitory $GABA_A$ receptors. Science. 269:977–981.
Stein V, Nicoll RA. 2003. GABA generates excitement. Neuron. 37:375–378.
Stevens JC, Green BG, Krimsley AS. 1977. Punctate pressure sensitivity: effects of skin temperature. Sen Processes. 3:238–243.
Sur M, Nelson RJ, Kaas JH. 1982. Representations of the body surface in cortical areas 3b and 1 of squirrel monkeys: comparisons with other primates. J Comp Neurol. 211:177–192.
Sur M, Wall JT, Kaas JH. 1984. Modular distribution of neurons with slowly adapting and rapidly adapting responses in area 3b of somatosensory cortex in monkeys. J Neurophysiol. 51:724–744.
Svensson P, Graven-Neilsen T, Arendt-Neilsen L. 1998. Mechanical hyperesthesia of human facial skin induced by tonic painful stimulation of jaw muscles. Pain. 74:93–100.
Szabadics J, Varga C, Molnar G, Olah S, Barzo P, Tamas G. 2006. Excitatory effect of GABAergic axo-axonic cells in cortical microcircuits. Science. 311:233–235.
Szolcsanyi J. 1987. Capsaicin and nociception. Acta Physiologica Hungarica. 69:323–332.
Taira T, Lamsa K, Kaila K. 1997. Posttetanic excitation mediated by $GABA_A$ receptors in rat CA1 pyramidal neurons. J Neurophysiol. 77:2213–2218.
Tommerdahl M, Delemos KA, Favorov OV, Metz CB, Vierck CJ, Jr, Whitsel BL. 1998. Response of anterior parietal cortex to different modes of same-site skin stimulation. J Neurophysiol. 80: 3272–3283.
Tommerdahl M, Delemos KA, Vierck CJ Jr, Favorov OV, Whitsel BL. 1996. Anterior parietal cortical response to tactile and skin-heating stimuli applied to the same skin site. J Neurophysiol. 75: 2662–2670.
Tommerdahl M, Whitsel BL, Favorov OV, Metz CB, O'Quinn BL. 1999. Responses of contralateral SI and SII in cat to same-site cutaneous flutter versus vibration. J Neurophysiol. 82:1982–1992.
Torebjork HE, Lundberg LE, LaMotte RH. 1992. Central changes in processing of mechanoreceptive input in capsaicin-inducted secondary hyperalgesia in humans. J Physiol. 448:765–780.
Tran TD, Hoshiyama M, Inui K, Kakigi R. 2003. Electrical-induced pain diminishes somato-sensory evoked magnetic cortical fields. Clin Neurophysiol. 114:1704–1714.
Vierck CJ Jr, Cannon RL, Fry G, Maixner W, Whitsel BL. 1997. Characteristics of temporal summation of second pain sensations elicited by brief contact of glabrous skin by a preheated thermode. J Neurophysiol. 78:992–1002.
Voipio J, Kaila K. 2000. GABAergic excitation and K^+-mediated volume transmission in the hippocampus. Prog In Brain Res. 125:329–338.
Walters RJ. 2004. Excitation and adrenaline: GABA—the bipolar neurotransmitter. Cellscience Reviews. Vol. 1, No. 1, ISSN. 1742—8130.
Whitsel BL, Favorov OV, Li Y, Lee J, Tommerdahl M. 2009. Nociceptor afferent drive alters SI neuron response to mechanical stimulation of the RF. Neurosci Abstr. 35:562.11.
Whitsel BL, Favorov OV, Li Y, Quibrera M, Tommerdahl M. 2009. Area 3a neuron response to skin nociceptor afferent drive. Cereb Cortex. 19:349–366.
Whitsel BL, Favorov OV, Tommerdahl M. 2000. Detection and measurement of the somatosensory cortical response to noxious skin stimulation using optical intrinsic signal (OIS) imaging. In: Casey KL, Bushnell MC, editors. Pain imaging. Chapter 3. IASP Press. p. 47–93.
Whitsel BL, Kelly EF, Delemos KA, Xu M, Quibrera PM. 2000. Stability of rapidly adapting afferent entrainment vs responsivity. Somatosens Mot Res. 17:13–31.
Whitsel BL, Kelly EF, Quibrera M, Tommerdahl M, Li Y, Favorov OV, Xu M, Metz CB. 2003. Time-dependence of SI RA neuron response to cutaneous flutter stimulation. Somatosens Mot Res. 20:45–69.
Whitsel BL, Kelly EF, Xu M, Tommerdahl M, Quibrera M. 2001. Frequency-dependent response of SI RA-class neurons to vibrotactile stimulation of the receptive field. Somatosens Mot Res. 18:263–285.